Effect of Macropores on Infiltration and Percolation: An Experimental Investigation

By

KALULI, J. Wambua

A thesis presented to the University of Ottawa in partial fulfillment of the requirements for the degree of Master of Applied Science in Civil Engineering

DEPARTMENT OF CIVIL ENGINEERING
UNIVERSITY OF OTTAWA
Ottawa, Ontario, Canada

March 1990

ISBN 0-315-60045-4

To my grandmother, Mutunge wa Nthuei

ABSTRACT

The importance of macropores in hydrology has been stressed recently because of the fact that they play an important role in the transportation of pollutants into the ground water reservoir. The purpose of this laboratory investigation was to study the effect of soil macropores (large non-capillary pores) on infiltration and percolation. This was done by measuring runoff, infiltration and tile flow rates for different macropore populations.

It was found that increasing macropore populations caused a change in infiltration parameters. The increase in percolation occurring as a result of increased number of macropores is associated with an increased bypass of the soil matrix by percolating water. The basic infiltration capacity increased with increasing number of macropores. This observation was used to develop the concept of macropore index (M-index), which could be adopted as a standard method for quantifying macropore populations in the soil.

Horton equation has been shown by workers such as Singh and Buapeng (1977) to produce better fit of field data than other empirical infiltration equations. However, in this work, the superiority of Horton equation has been observed only with respect to the simulation of cumulative infiltration. Philip and Kostiakov equations simulate instantaneous infiltration more accurately than Horton equation, but since in practice infiltrated volume is of more interest than instantaneous infiltration rate, Horton equation remains more acceptable than Philip and Kostiakov equations. In this work, some modifications have been suggested for the latter two equations. The performance of the modified equations is comparable to that of Horton equation.

In situations where soil M-index changes seasonally, it becomes difficult

for appropriate equation parameters to be determined accurately. To enable Horton equation to calculate infiltration in macroporous conditions, an improved form has been suggested.

The influence of increasing the population of macropores on surface runoff and tile flow has been investigated. Results of this work indicate that hydrologic models, taking infiltration and percolation into account, should consider the influence of macropores where the populations of the latter are likely to change significantly from time to time.

ACKNOWLEDGEMENTS

The author is grateful for the technical guidance, encouragement and support of Dr. Richard Warnock throughout this research project. In addition, the technical support and assistance with laboratory analysis given by Robert Moore and Richard Moore is greatly appreciated.

Deep appreciation is expressed to CIDA and the Government of Kenya for providing financial assistance. The author also appreciates the effort made by Prof. D.B Thomas, of Nairobi University in summer 1988, to expose him to Kenya's Soil and Water Conservation research needs. This made it possible for the author to carry out this research with Kenya's needs in mind.

Finally, I am very grateful to my wife Mwikali for giving me loving, prayerful, support without which it would have been impossible to complete this work.

Contents

List of Figures

List of Tables

NOTATIONS

A	Empirical constant in Philip and Kostiakov equations
B	Empirical constant in Philip and Kostiakov equations
C	Specific moisture
C'	A coefficient in modified Kostiakov equation
D	A coefficient in modified Philip equation
E	Fitting efficiency
ET	Evapotranspiration
F	Cumulative infiltration
F'	Calculated cumulative infiltration
f_c	Basic infiltration capacity
f	Observed infiltration capacity at time t
f'	Calculated infiltration capacity
h	Hydraulic head
i	Hydraulic gradient
k	Empirical constant in Horton equation
K	Saturated hydraulic conductivity
$\bar{K}$	Saturated hydraulic conductivity at natural saturation
$M - index$	Macropore index
n	A symbol for porosity or macropore index
P	Percolation
Pd	Drainable porosity

q	Discharge flux
Q	Discharge
R^2	Correlation coefficient
Re	Reynold's number
Ro	Runoff rate
S	Soil sorptivity
$S\&P$	Seepage and Percolation
V	Velocity
z	Elevation above a datum
α	A constant in modified Horton equation
θ	Moisture content
θ'	Degree of saturation
ψ	Pressure head
$C(\theta)$	Specific moisture capacity a function of Moisture content
$C(\psi)$	Specific moisture capacity a function of pressure head
$D(\theta)$	Soil water diffusivity a function of Moisture content
$D(\psi)$	Soil water diffusivity a function of pressure head
$K(\theta)$	Hydraulic conductivity a function of Moisture content
$K(\psi)$	Hydraulic conductivity a function of pressure head

Chapter 1

INTRODUCTION

1.1 Motivation and Scope

Infiltration and percolation are important processes in hydrology. While infiltration is the process by which water enters the soil matrix from the ground surface, percolation is visualized as the downward movement of water through the soil towards the water table (Yoder, 1986). Macropores, which are non-capillary pores that occur in soil providing channels that permit preferential water flow in the soil (Beven and Germann, 1982) have a major impact on infiltration and percolation. The need to be able to model hydrologic processes such as surface runoff, sheet erosion, water table elevations, pollution of ground water by agricultural chemicals and to design irrigation and drainage systems properly in spite of the presence of macropores was the main motivation for this research.

Under macroporous conditions, the wetting front of infiltrating water is not well defined. Instead, water follows channels of least resistance. Non-capillary channels are more common in soils that are seldom disturbed, such as forested areas. Such channels, which are likely to form after roots decompose, can complicate design of drainage structures. Nelson and Gregory (1988) found that flow through large non-capillary channels was more significant in areas where trees have grown for a longer period. Since infiltration and percolation change significantly with the introduction of macropores, over-design of surface drainage systems in forested areas could result when infiltration information prior to the development of the forest is used.

Macropores not only increase the area where infiltration can take place, but also shorten the path of water to the ground water table or tile drains. The importance of macropores depends on the purpose for which a knowledge of infiltration is required. For example, infiltration rates should be more precisely known for the design of an irrigation project in a farm, than in the calculation of excess rainfall in a watershed by the SCS method. The latter method lumps infiltration together with interception and depression storage to form initial abstraction.

In soil, there are two possible domains of flow. Water can either infiltrate through the soil matrix or flow through the non-capillary pores by gravity (Beven and Germann, 1982). Flow through macropores is referred to as "bypass" since water bypasses the soil matrix. Bypass flow can only take place when rainfall intensity exceeds soil infiltration capacity. In such a condition ponding occurs (Edwards et al, 1979). It is only holes and cracks open to the surface that can take water by non-capillary movement. Shirmohammadi et al, (1989) observed that the concept of bypass flow through macropores and the fact that they allow fast movement of water and chemicals goes back to studies by Schumacher (1864) who observed that infiltration is mainly controlled by large pores.

Shirmohammadi and Skaggs (1985) have indicated that decomposition of roots increases the hydraulic conductivity of soil and that using the original saturated hydraulic conductivity instead of increased conductivity values during the growing season in the Green-Ampt infiltration equation resulted in significant underestimation of infiltration. In agricultural fields, the hydrologic characteristics of the soil are likely to change from time to time. The influence of cracks is also likely to vary seasonally. Good knowledge about these variations is required in order to model infiltration and transportation of chemicals in the soil.

The best known physically based infiltration model is Richards' equation, which is based on Darcy's law. The presence of macropores in the soil causes Darcy's law not to be applicable meaning that Richards' equation may not produce an accurate analytical solution in the presence of macropores. In such conditions empirical equations might perform more satisfactorily than the physically based equations. Empirical equations, which are more commonly used in practice, include Horton, Philip and Kostiakov equations. Singh and Buapeng (1977) showed that Horton equation was better in modelling infiltration than Kostiakov and Philip equation. Using the infiltration data obtained in this research a comparison has been carried out between these equations.

Since the surface of a small watershed such as a farm is always changing due to seasonal changes in moisture, vegetation, and soil structure, the parameters of infiltration equations should be adjusted to reflect these changes, otherwise the equations would produce inaccurate simulations. There is also need to have a method of quantifying variations in macropore populations, particularly in situations where there are frequent changes.

The results presented in chapter 6 are based on laboratory investigation. Infiltration and tile flow data were collected from a soil bed for different densities of idealized macropores. The soil bed used in this work could only contain 50 cm depth of soil. This is different from a typical natural soil profile for which the saturated hydraulic conductivity is often assumed to be equal to the basic infiltration capacity (Skaggs and Miller, 1977). This approximation is often made when it is not convenient to measure hydraulic conductivity separately. The fact that the soil profile used in the laboratory is so shallow may invalidate this assumption.

The laboratory investigation provided controlled conditions and made it possible to vary macropore populations more precisely and in a measurable pattern. In the laboratory, it was possible to produce rainfall of a fixed intensity. Analysis of the collected data will yield a better understanding of the impact of macropores on infiltration and percolation which will assist modellers of these hydrologic processes.

1.2 Objectives

The objectives of this study are

1. To use a finite difference simulation to determine the importance of an impermeable barrier close to the soil surface, as was the case in the experimental equipment.
2. To examine the way equation parameters change with the introduction of macropores and consequently determine a way to modify the equations to be of use in changing macroporosity.
3. To determine a method of quantifying macropore populations for the purposes of modelling infiltration and other hydrologic processes.
4. To compare the accuracy of the three equations to simulate infiltration for the conditions of the study. This would make it possible check the claim in literature that Horton equation is the best empirical infiltration equation.
5. To demonstrate the effect of macropores on surface runoff and tile flow and consequently show the effect of ignoring macropores on the performance of hydrologic simulation models.

Chapter 2

LITERATURE REVIEW

2.1 Modelling Infiltration

Infiltration is the process by which water enters the soil matrix from the ground surface. It occurs at a rate that decreases with time. For a given soil there is a limiting curve, called soil infiltration capacity curve (see Figure 2.1), that defines the maximum possible rate of infiltration at any time. Infiltration capacity decreases with time after the onset of water application, and finally reaches an approximately constant value. The decline is usually associated with the filling up of soil pores with water. Clay soils exhibit more rapid declines than light textured sandy soils that have large pores (Freeze and Cherry, 1979). If the infiltration rate is exceeded by the water application rate, ponding takes place and, consequently, there may be overland flow. Figure 2.2 shows four moisture zones that may occur during infiltration. There may exist a saturated zone near the soil surface followed by a transmission zone of unsaturated flow and fairly uniform moisture content.

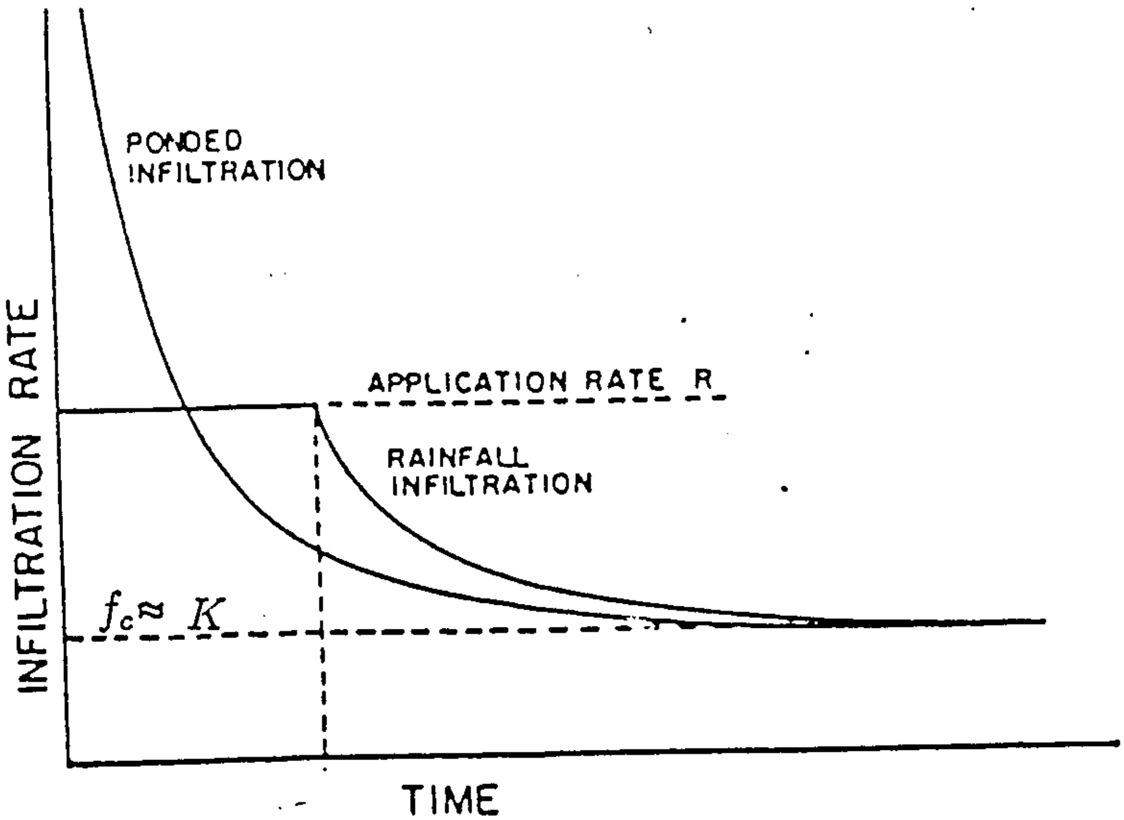

Figure 2.1: Infiltration Rate Variation with Time (after Skaggs and Miller, 1983)

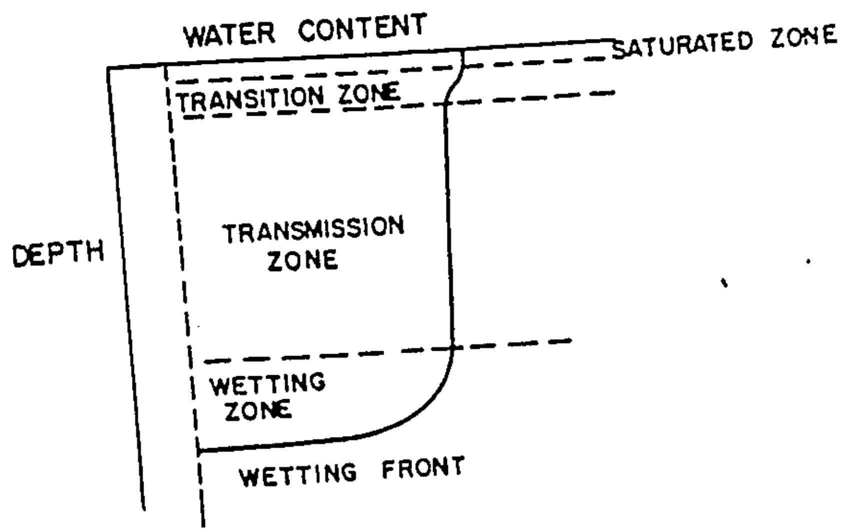

Figure 2.2: Moisture Zones During Infiltration

The wetting zone has moisture that decreases with depth while at the wetting front the change of moisture content with depth is so great that it gives the appearance of a sharp discontinuity between the wet soil above and the dry soil below. The depth penetrated by the wetting front depends on the amount of infiltration and the physical properties of the soil. It may be only a few centimeters in one soil and several in another (Chow et al, 1988).

Infiltration equations are used to simulate infiltration quantities, either for hydrologic modelling or engineering planning and design. Richards' equation, which is further discussed in chapter 3, is the best known physically based infiltration equation. Other physically based equations such as Green-Ampt equations are either related or simplifications of Richard's equation. The most frequently used infiltration equations are empirical. Horton, Philip, Kostiakov and Holtan equations are discussed in detail below.

2.1.1 Horton Equation

Making use of some experimental data, Horton (1940) proposed the equation,

$$f = f_c + (f_o - f_c)e^{-kt} \tag{2.1}$$

where

f_o = initial infiltration capacity (mm/hr).

f = the infiltration capacity at time t (mm/hr).

f_c = final or equilibrium infiltration capacity (mm/hr).

k = an exponent governing the rate of decline of the infiltration capacity.

Cumulative infiltration "F" is given by Horton equation as:

$$F = f_c t - \frac{f_o - f_c}{k}(e^{-kt} - 1) \tag{2.2}$$

Irrig.	Field	*Horton*		*Kosti.*		*Modi. Kosti.*	
#	data	F	% error	F	% error	F	% error
8	90.2	69.8	23	77.06	15	78.88	13
10	42.89	42.74	0.3	41.09	4	45.00	5
11	65.7	83.53	27	97.27	48	95.62	46
15	66.8	69.06	3	62.11	7	60.28	10

Table 2.1: Final Infiltrated Volume (cu ft/ft) (after Turbak and Morel-Seytoux, 1988)

Since the infiltration capacity f is expressed as a function of time rather than of soil water content, the equation holds true only if throughout the period of simulation rainfall intensity is high enough to cause ponding; otherwise, f is equated to rainfall intensity. Horton equation does not account for variation in antecedent moisture conditions. This is its greatest weakness.

Carrying out comparisons of different equations Singh and Buapeng (1977) found that Horton equation performed better than ϕ-index, Kostiakov and Philip methods in determining rainfall excess. Philip and Kostiakov equations were found to be comparable but ϕ - index method performed very poorly.

Turbak and Morel-Seytoux (1988) used Horton equation for modelling border irrigation. Table 2.1 shows the simulated and observed infiltrated volumes of water. Comparing observed and simulated quantities of infiltration, it is clear that the errors made by using Horton equation are generally smaller than those made by using Kostiakov equations.

Morin and Benyamini (1977) modified Horton equation to simulate infiltration through a soil crust. It is as follows.

$$f = f_c + (f_o - f_c)e^{-\gamma p t} \tag{2.3}$$

Symbols, f_o, f_c, f and t have the same meaning as in the regular Horton equation. Symbol γ is a coefficient related to rain drop size. The rainfall intensity is represented by p. From some tests done, it was found that uncrusted dry soil gave the highest f_o and the lowest γ while crusted soil gave the lowest f_o and the highest γ values. Crusted soil with a dry surface gave values of f_o and γ between the values in the former two cases respectively (Morin and Benyamini, 1977).

Research done with Horton equation indicates that it is a reliable equation for simulation of infiltration volumes, which might explain its popularity. This equation has been further compared with other equations in chapter 6 of this thesis.

2.1.2 Kostiakov Equation

The cumulative infiltration form of Kostiakov equation as presented by Clemens (1983) is

$$\begin{aligned} F &= \frac{A}{B+1}t^{B+1} \\ \frac{dF}{dt} &= f = At^B \end{aligned} \tag{2.4}$$

where F and f are cumulative infiltration and instantaneous infiltration capacity respectively. A and B are empirical constants. This empirical infiltration equation is popular in irrigation applications because it is simple and fits data sufficiently. The parameters above are dependent on soil properties and the duration of infiltration time. They are fairly easy to determine from observed data (Clemens 1983).

Over short time periods this equation fits a wide variety of infiltration data reasonably well. However, over long time periods, the resulting infiltration capacity approaches zero while in actual fact the ultimate infiltration rate approaches a certain constant. In an attempt to solve this problem, Clemens and Dedrick (1980) developed the Kostiakov branch equation which states that,

$$\begin{gathered}
\text{for } t \leq t_c \text{ then, } F = \tfrac{A}{B+1} t^{B+1} \text{ and} \\
\text{for } t \geq t_c;\ F = \tfrac{A}{B+1}(-B) t_c^{B+1} + f_c t \\
\text{or for } t \leq t_c;\ f = At^B \text{ and} \\
\text{for } t \geq t_c;\ f = f_c \\
\text{At } t = t_c\ ,\ f_c = At_c^B, \text{ and this defines } t_c.
\end{gathered}$$

Determining the constants for the branch Kostiakov equation is more difficult than with the simple Kostiakov formulation (Clemens, 1983). This form of Kostiakov equation has not been applied much.

2.1.3 Philip Equation

Philip (1957) come up with an equation which assumes immediate surface ponding.

$$F = St^{\frac{1}{2}} + At + Bt^{\frac{3}{2}} + \ldots\ldots \tag{2.5}$$

The equation is usually written with only two terms

$$F = St^{\frac{1}{2}} + At$$

$$f = \frac{1}{2}St^{\frac{-1}{2}} + A \qquad (2.6)$$

Parameter S, called sorptivity, determines the amount of moisture absorbed in the absence of gravitational effects. For large values of t, the infiltration capacity f in an infiltration event should be equal to ultimate infiltration rate f_c. It follows that $A = f_c = K$ (saturated hydraulic conductivity). However, this is not yet a firmly accepted fact. Some researchers think A can take on a value different from f_c (Knight, 1983). Philip and Frollell (1964) stated that the term At consists essentially of that contribution to infiltration arising from gravity. Sorptivity S was first introduced by Philip (1957). Since it is a function of moisture content, it is often written as $S(\theta)$. It is a measure of water absorption by soil without gravitational effects. This is one of the most important soil parameters governing the early portion of infiltration (Chong and Green, 1983). Sorptivity varies for different soils and depends upon the structure and the antecedent water content of the soil.

Coefficients S, A, and B in equation 2.7 are all functions of water content (Chong and Green, 1983). If water diffusivity $D(\theta)$ and hydraulic conductivity $K(\theta)$ are known, then the values of S, A, etc can be found numerically. However, it is a very tedious job to measure $D(\theta)$ and $K(\theta)$. Chong and Green (1983) reported that a simpler method for measuring these factors was suggested by Talsma (1969). Assuming that the early portion of infiltration can be described by equations 2.8 and 2.9, the value of S can be estimated from the slope of the plot of the cumulative infiltration F versus the square root of elapsed time.

$$f = 0.5St^{\frac{-1}{2}} \qquad (2.7)$$

$$F = St^{\frac{1}{2}} \qquad (2.8)$$

Sorptivity varies in a given area from place to place and is log-normally distributed in a large area (Chong and Green, 1983). There exists a mathematical relationship between S and saturated hydraulic conductivity K.

$$S = 6.3(\theta_s - \theta)^{0.5} K^{-0.25} \tag{2.9}$$

However this relationship has not yet been tested with field measurements (Chong and Green, 1983), so it cannot be used with confidence.

2.1.4 Holtan Equation

Holtan equation, which closely resembles Horton equation, defines the infiltration capacity f at time t given by,

$$f = a(\theta_{su} - \theta)^{1.4} + f_c \tag{2.10}$$

Parameter a is an index of surface-connected porosity which is a function of the surface conditions and the plant roots (Paine and Watt, 1988, Bauer, 1974), θ_{su} is the saturated volumetric moisture content in the upper soil layer, while θ is the moisture content. A low value of initial moisture content will lead to a greater volume of water infiltrating before runoff takes place. Parameter f_c represents the ultimate infiltration capacity. A low value of f_c prevents infiltration from taking place. Instead of using quantity 1.4, a varying factor n which varies with the soil studied is sometimes used (Bauer, 1974).The Holtan equation has the advantage that it gives f as a function of antecedent moisture condition while Horton gives f as a function of time. One disadvantages of this equation is that one has to keep track of moisture content variation, and this is expensive. Failure to use the correct value of θ could cause large errors in computed infiltration.

Holtan equation, which is not used much for modelling purposes, has been applied by Paine and Watt (1988) in their model TILE. This equation will not be discussed any further in this thesis since it involves values of moisture content the time variation of which was not monitored in the experimental work.

Some other methods used in determination of infiltration loss are the SCS method and the Green-Ampt method. The latter method has been featured a lot lately in literature. It is popular in research since it is more physically based than most of the other more frequently used equations.

2.2 Percolation

Percolation is often lumped with seepage and together referred to as seepage and percolation (S&P). While percolation is visualized as the downward movement of water through the soil towards the water table, seepage is understood to be the lateral movement of water in saturated soil (Yoder, 1986). Paine and Watt (1988), in their development of TILE model, refer to percolation as the movement of water from the upper soil layer to the lower layer. The upper layer is considered to be between 20 and 40 cm thick. Prior to any percolation, the field capacity of the upper zone must be satisfied.

In the TILE model, percolation P is given as;

$$P = \frac{\theta_u - \theta_{fu}}{\theta_{us} - \theta_{fu}} f_c. \tag{2.11}$$

- θ_u= upper moisture content
- θ_{fu} = upper field capacity (FC)
- θ_{us} = upper zone saturation moisture content
- f_c = basic infiltration capacity

Once the field capacity has been reached, excess water is added to the ground water table and subsequently released to the drains, if drainage is provided for.

Yoder (1986) studied seepage and percolation (S&P) in the context of basin irrigation of rice in the hills of Nepal. The irrigation basins have a puddled top layer which should be left saturated. It is puddled in order that its permeability may be lowered and maintain a pond of water. To simulate the rice growing conditions, measurement of percolation is often done in a lysimeter. The percolate collected at the bottom of the lysimeter tank gives a measure of percolation. This method has the disadvantage that the discontinuities produced by the walls of the tank create a condition different from the natural condition. Also, as the soil is put in the lysimeter tanks, it is disturbed and is no longer the same as the undisturbed soil (Yoder, 1986). He recommends a mass balance method of percolation measurement where

$$W = I + Rn - ET - S\&P - Ro \tag{2.12}$$

This formula can give a more reasonable estimate of S&P. The measurement is weighted over a larger area.
W = observed water surface subsidence in the paddy field.
I = irrigation depth
ET = evapotranspiration
S&P = seepage and percolation
Ro = Runoff
Rn = rainfall
The units of all the components of the equation are millimeters (mm). The components of the mass balance equation that cannot be measured directly, such as ET, are approximated using well-established procedures.

Assuming that the interface between the less permeable top layer and the lower one is at atmospheric pressure, Yoder (1986) suggests that Darcy's law could be applied for the one-dimensional vertical flow.

$$q_z = -K(H + z)/z \tag{2.13}$$

q_z = volume flux (mm/day)
K = saturated hydraulic conductivity (mm/day)
H = hydraulic head above the soil (mm)
From equation 2.13, it can be seen that when the depth (z) of the puddled layer is small, then volume flux is high. Percolation losses will be higher. Leaving a clay surface dry for a long time will cause formation of cracks. In cases where there are large volume of macropores, most of the water could seep through the cracks and bypass the soil matrix, hence causing the bulk of the soil not to acquire the required moisture.

Yoder (1986) reported that in the hills of Nepal, there seems to be a significant change of hydraulic conductivity during the growing season and consequently higher percolation losses. The increase in percolation is noted to be greatest where rotation irrigation is practiced. In this case, when the soil is left dry, the clay in the top layer shrinks and forms cracks through which large volumes of water can seep in the following irrigation event. Cracking is often associated with soils rich in montimorillonite or vermiculite minerals (Hausenbuiller, 1980). In wet conditions, these minerals swell, while in dry conditions, shrinkage and hence cracking take place.

Adhikari (1986) explains that plant roots and crop residual may create preferential paths. The residual, after decomposing, may create paths through which water may pass preferentially, and in the process erode the passage, causing enlargement of the channels and hence percolation may increase during the growing season.

In the absence of tillage, cracks formed may be irreversible. The lines of cleavage remain intact and so the cracks can only increase in size. This could explain why there is an increase in saturated hydraulic conductivity during the growing season.

The average drainable porosity represents the specific yield, or the maximum water available through gravity (Paine and Watt, 1988). Soil with a large drainable porosity is likely to experience large percolation rates. Paine and Watt (1988) present the method of measuring drainable porosity from field drainage data, first suggested by Taylor (1960). It involves the integration of the recession limb of the tile discharge hydrograph and relating this volume to the drop in ground water table for the same period of time. Drainable porosity is the ratio of the sum of volume of water drained and the sum of evaporation and transpiration (often known as evapotranspiration) to the volume of soil drained.

2.3 Tiled Field Simulation Model (TILE)

A computer coded tiled field simulation model called TILE model was developed by Paine et al (1988). It is a physically based model designed to simulate the hydrologic response of an agricultural field subjected to tile drainage. Infiltration, filling of depression storage and percolation are modelled.

TILE simulates hydraulic responses on an hourly basis. The available components are surface drainage, soil moisture, water-table elevation, tile flow and evapotranspiration analyses. Details of formulas and calculations are available elsewhere (Paine and Watt, 1988). The Holtan equation (discussed earlier in chapter 2) is used to compute infiltration capacity in mm/hr. Equation 2.11 is used to compute percolation.

Thornthwaite's equation (Thorntwaite and Holzman, 1942) is used to calculate evapotranspiration from depression storage and the soil surface. Temperature data is the main requirement for this equation.

For the model to run, field data and event data have to be input into special files. The parameters required to represent field conditions are field, soil, and evapotranspiration description parameters (Paine et al, 1988). Initial soil water content is very important. Field description parameters include field slope and length, tile diameter and effective radius, spacing, number of rows and length of tile laterals. Soil description consists of hydraulic conductivity, the depth to the impermeable layer, a flux coefficient, drainable porosity and an estimate of the depression storage. Hourly rainfall and temperature data describe the event.

The model shows different levels of sensitivity to the different parameters put in. Its output is particularly sensitive to variation in the initial moisture content prior to a rainfall event. This is more so in soils with low drainable porosity. Doubling hydraulic conductivity approximately increases tile flow volume by about 20 %. Drainable porosity, depth to the impermeable layer and depth of the upper soil zone are other parameters to which the model is sensitive. Computed tile flow as well as runoff will be affected by changes in any of these parameters.

A lower basic infiltration capacity f_c will prevent excess moisture from entering the soil. Variation in f_c will affect peak flows, total volume of tile flow and the shape of tile discharge hydrograph. The model has been noted not to be very sensitive to this parameter so when hydraulic conductivity is known, it is equated to the latter.

Table 2.2 identifies the key model parameters and suggests their method of estimation for un-calibrated fields. Macropores, described in more detail

Table 2.2: Estimation of Tile Model Parameters (after Paine and Watt, 1988)

Symbol	Name & Description	Typical Range	Method of Estimation
L_s	Drain spacing, m	5-20	Measurement
n_r	Number of rows of lateral tile drains		Measurement
L_t	Equivalent length of tile laterals for rectangular layout, m		Measurement or calculation
K_s	Hydraulic conductivity, m/day	0.1-10	Measurement or literature
D_i	Depth to impermeable barrier from drain axis, m	0.5-5	Measurement or literature
C	Average flux coefficient	0.8-1.0	Use 0.9
μ	Drainable porosity	0.01-0.05	Measurement or literature
D_{max}	Maximum depression storage, mm	1-10	Literature
θ_{fu}	Field capacity of upper layer	0-1.0	Measurement or literature
h_u	Depth of upper layer, mm	0-300	Measurement
a	Vegetation parameter in Holtan's equation	0.1-1.0	Literature

in the section below, when present in the soil could affect the values of the TILE parameters causing the simulations made by the model to be far from accurate. This is demonstrated in this work.

2.4 Nature of Macropores

Macropores provide preferential paths, permitting non-equilibrium flow (Beven and German, 1982). In non-equilibrium flow the linear Darcy's law does not hold. The flow could be either non-linear and laminar or even turbulent. In such conditions the hydraulic gradient could be greater than 1 while Reynolds number is greater than 10 (Freeze and Cherry, 1979). Reynolds number R_e is a dimensionless number that expresses the ratio of inertial to viscous forces during flow. Reynolds number for flow through porous media is defined as

$$R_e = \frac{\rho v d}{\mu}$$

where ρ and μ are fluid density and viscosity, v the specific discharge, and d a representative length for the porous medium. The representative length is taken as the mean pore dimension or the mean grain diameter. In the case of macropores d would be the average pore diameter. Figure 2.3 shows the range of validity of Darcy's law. Preferential flow only lasts a short time after input at the soil surface has ceased. The presence of macropores in the soil presents a serious difficulty in attempting the simulation of infiltration with simple infiltration formulae.

The shape of macropores varies from planar slots (cracks or fissures) through voids of irregular cross-section known as vughs to cylindrical pipes. Anything or process that creates cavities, tubes or cracks in the soil is a means of creating macropores. Soil fauna are often responsible for the

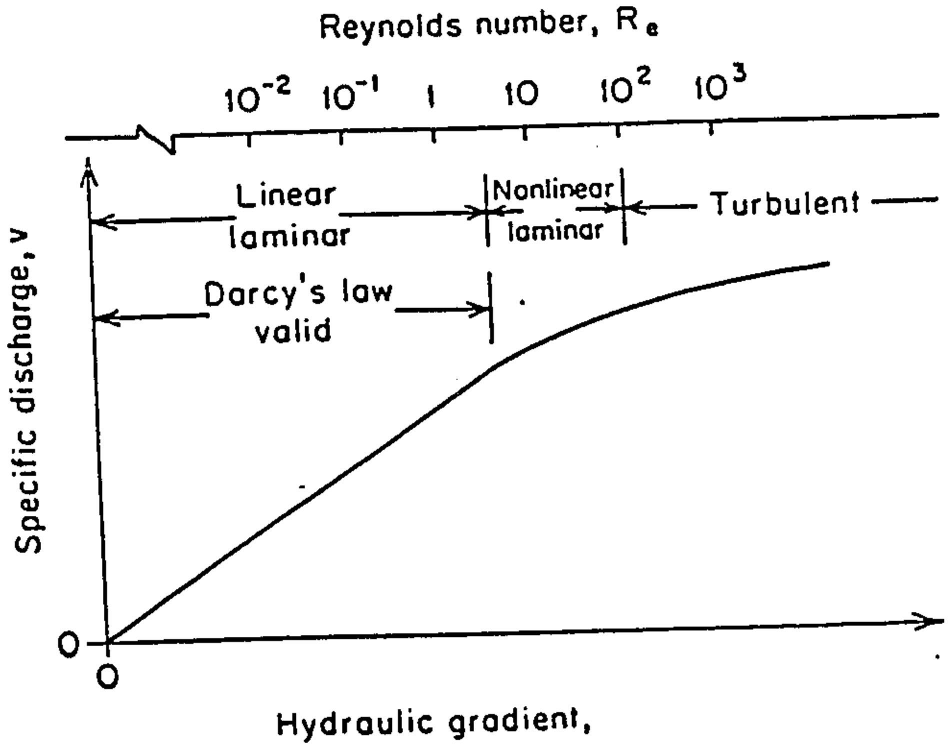

Figure 2.3: Validity Range of Darcy's Law (after Freeze and Cherry, 1979)

formation of tubular macropores of sizes between 1 and 50 mm. Such macropores are concentrated near the soil surface.

When roots decay, tubular macropores taking the shape of the root usually develop. Nelson and Gregory (1988) found that as trees in forested areas grow older, and some are harvested, roots will provide additional non-capillary pores when they decompose. Macropores have a very dynamic nature. Their quantity and quality are likely to change a lot depending on the treatment of the soil. The volume of macropores depends on the dynamic balance between constructive and destructive processes, one of which is tillage (Beven and German, 1982). Even though tillage and sub-soiling will generally decrease the soil bulk density and increase its porosity, the resulting destruction of macropores affects infiltration patterns significantly. For example, the abundance of earthworm burrows is less in cultivated than in uncultivated soil (White, 1985).

Cracks and fissures are macropores that may be formed by either shrinkage resulting from desiccation of clay or chemical weathering of bed-rock. Soil shrinkage and swelling usually result in cracking. Piping caused by sub-surface flow erosion cause another category of macropores that occur in highly permeable and non-cohesive soils (Beven and German, 1982).

Sub-surface ground water flow has been noted to be affected by the presence of macropores. In the presence of macropores, Edwards et al (1979) noticed that the rising side of the tile drain hydrograph is almost instantaneous. In cracked soil, the response of the tile drains to intense rainfall is faster than the case where there are no cracks. For cracked soil, the peak tile flow seems to coincide with peak rainfall. In the absence of cracks, peak tile flow occurs much later, after the rainfall event. The fact that macropores change the rate of water flow into the ground is an indicator that their presence could affect the rate of transport to ground water of agricultural chemicals applied at the surface.

Using numerical models, Edward et al (1979) showed that surface-connected macropores effectively transmit water when more water is applied to the soil surface than can infiltrate by capillary action. Infiltration and runoff depend on the number of macropores per unit surface area. With the help of experiments, infiltration and redistribution of water in soils containing macropores has been shown not to be adequately described by theories that treat the soil as a homogeneous medium conforming to Darcian principles of water flow (White, 1985).

Introduction of macropores into soil causes a sharp change in hydraulic conductivity (Beven, 1981). Macroporosity is associated with the pore volume that drains at a tension of 0.05 bar. In other words, water in macropores drains by gravity (White, 1985). Even though macropores may comprise only a small percentage of the total soil volume, their effect on infiltration and redistribution of water in the soil can be profound.

The subject of preferential transport of water and solutes has drawn the attention of researchers in the recent years because of the possible pollution of ground water by the rapid leaching of chemicals (Bouma et al, 1983). There is a growing concern for ground water pollution particularly from agricultural chemicals. The main agricultural pollutants include fertilizers, pesticides, and herbicides. Field experiments have shown that undisturbed soil conducts solutes at a rate faster than expected (Kissel et al, 1973). This is in contradiction to an earlier assumption that an non-reactive solute moves through the medium at the same velocity as the water and that all resident water and solutes are displaced by the incoming water. However, in soil with macropores only partial displacement of resident water takes place (White, 1985). This kind of displacement is referred to as channeling, bypassing or preferential flow (Scotter, 1978, Beven and Germann, 1982).

The presence of macropores can either increase or decrease the quantity of solutes leached depending on the following (White, 1985).

1. The location of the solute. Solute is more easily leached if it is right on the soil surface.
2. The ratio of macropore to matrix flow . This could be difficult to determine.
3. The saturated hydraulic conductivity of the matrix.
4. Soil antecedent water content.
5. The contact area between bypassing flow and the relatively static water of the matrix.
6. The rate of solute diffusion between the mobile and immobile water volumes.

The topic of transport of solutes in soil will not be considered in the thesis, but an understanding of it helps to understand the action of macropores.

The literature covered indicates that Horton equation gives a better fit of field infiltration data than Kostiakov and Philip equations. However nobody, including Singh and Buapeng (1977), has explained why its performance seems to be better than that of other empirical infiltration equations. In this thesis the performance of Horton, Kostiakov and Philip equations will be compared. An attempt is made to show possible modifications on Philip and Kostiakov equations that would give them a performance comparable to that of Horton equation.

Macropores have been found not only to accelerate the movement of water in soil, but also to increase the accessibility of pollutants to ground water. This creates a need to acquire more information to enable hydrologic modelling even in the presence of macropores. There is a need for a method of quantifying macropore populations, and such a method will be suggested.

As a result of the influence of macropores the performance of infiltration equations is likely to be affected. It is the purpose of this thesis to show how equation parameters change with increasing macropore populations and suggest possible modification of the equations to enable modelling of infiltration even in the presence of macropores. The effect of macropores on tile flow will also be examined. As well, the effect of having an impermeable barrier close to the soil surface will be studied.

Chapter 3

THEORETICAL BACKGROUND

Before presenting the methodology and the results from this laboratory investigation, a number of concepts need to be introduced to the reader. This background is necessary to facilitate an understanding of the following chapters.

3.1 Soil Properties and Infiltration

The effect of soil properties on infiltration are clearly expressed by Richards equation which describes the physical processes that govern flow through soil is presented in this chapter even though it is not used in the analysis of the experimental data. The basic law of flow is Darcy's law which, when combined with a continuity equation that describes the conservation of fluid mass during flow through a porous medium, results in Richards' equation.

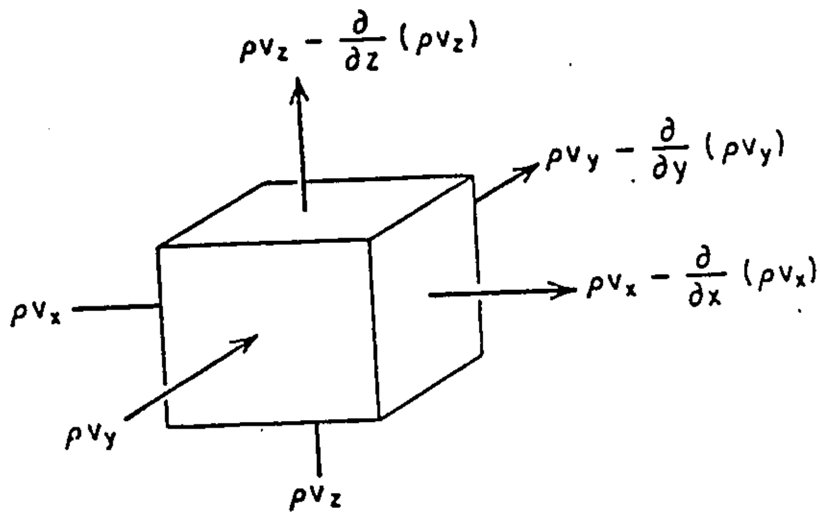

Figure 3.1: Elemental Control Volume

Considering an elemental control volume (unit volume) of porous media (soil) such as shown in Figure 3.1, the required relationship can be developed. The law of conservation of mass in a partially saturated medium requires that the net rate of fluid mass flow into any elemental control volume be equal to the time rate change of fluid mass within the element (Freeze and Cherry (1979)).

$$-\frac{\partial(\rho V_x)}{\partial x} - \frac{\partial(\rho V_y)}{\partial y} - \frac{\partial(\rho V_z)}{\partial z} = \frac{\partial(\rho\theta' n)}{\partial t} \tag{3.1}$$

$$\frac{\partial(\rho\theta' n)}{\partial t} = n\theta'\frac{\partial \rho}{\partial t} + \rho\theta'\frac{\partial n}{\partial t} + \rho n\frac{\partial \theta'}{\partial t} \tag{3.2}$$

The terms θ' and n denote the degree of saturation and porosity respectively. The degree of saturation is the ratio of volumetric moisture content θ to soil porosity n.

Darcy's law states that flow velocity V_z is related to hydraulic head h as follows;

$$V_z = -K(\psi)\frac{\partial h}{\partial z} \tag{3.3}$$

where $K(\psi)$ is the unsaturated hydraulic conductivity and z is the elevation with respect to a datum taken at the soil surface for the point under consideration. The ratio $\partial h/\partial z$ is the hydraulic gradient at the point being considered.

Hydraulic conductivity $K(\psi)$ is not only a function of pressure head but also of soil water content θ. Pressure head is the fluid pressure divided by the fluid unit weight. When pressure head is negative, which occurs when the soil is unsaturated, the pressure head is referred to as suction pressure (Freeze and Cherry, 1979).

Neglecting the first two terms on the right hand side of equation 3.2 and then combining equations 3.1 and 3.2, the following equation is obtained.

$$-\frac{\partial(\rho V_x)}{\partial x} - \frac{\partial(\rho V_y)}{\partial y} - \frac{\partial(\rho V_z)}{\partial z} = \rho n\frac{\partial \theta'}{\partial t} \tag{3.4}$$

Since

$$\theta = \theta' n \tag{3.5}$$

it follows that

$$-\frac{\partial(\rho V_x)}{\partial x} - \frac{\partial(\rho V_y)}{\partial y} - \frac{\partial(\rho V_z)}{\partial z} = \rho\frac{\partial \theta}{\partial t} \tag{3.6}$$

Applying equation 3.3 in equation 3.6,

$$\frac{\partial}{\partial x}\{K(\psi)\frac{\partial h}{\partial x}\} + \frac{\partial}{\partial y}\{K(\psi)\frac{\partial h}{\partial y}\} + \frac{\partial}{\partial z}\{K(\psi)\frac{\partial h}{\partial z}\} = \frac{\partial \theta}{\partial t} \tag{3.7}$$

Hydraulic head h is related to both z and pressure head ψ according to the following equation.

$$\psi = h + z \tag{3.8}$$

Taking equation 3.8 into account,

$$\frac{\partial h}{\partial x} = \frac{\partial h}{\partial \psi}\frac{\partial \psi}{\partial x} = \frac{\partial(\psi - z)}{\partial \psi}\frac{\partial \psi}{\partial x} = \frac{\partial \psi}{\partial x} \tag{3.9}$$

$$\frac{\partial h}{\partial y} = \frac{\partial \psi}{\partial y} \tag{3.10}$$

$$\frac{\partial h}{\partial z} = \frac{\partial(\psi - z)}{\partial z}\frac{\partial \psi}{\partial \psi} = (\frac{\partial \psi}{\partial z} - 1) \tag{3.11}$$

$$\frac{\partial}{\partial x}\{K(\psi\frac{\partial \psi}{\partial x}\} + \frac{\partial}{\partial y}\{K(\psi\frac{\partial \psi}{\partial y}\} + \frac{\partial}{\partial z}\{K(\psi\frac{\partial \psi}{\partial z} - 1\} = \frac{\partial \theta}{\partial \psi}\frac{\partial \psi}{\partial t} \tag{3.12}$$

$$\frac{\partial}{\partial x}\{K(\psi\frac{\partial \psi}{\partial x}\} + \frac{\partial}{\partial y}\{K(\psi\frac{\partial \psi}{\partial y}\} + \frac{\partial}{\partial z}\{K(\psi\frac{\partial \psi}{\partial z} - 1\} = C(\psi)\frac{\partial \psi}{\partial t} \tag{3.13}$$

$C(\psi)$ is the specific moisture capacity. It is the slope of the characteristic curve, and it represents the unsaturated storage property of the soil.

$$C(\psi) = \frac{\partial \theta}{\partial \psi} \tag{3.14}$$

$$\frac{K(\psi)}{C(\psi)} = D(\psi) \tag{3.15}$$

$D(\psi)$ is soil water diffusivity.

The one-dimensional ψ-based form of Richards' equation is given as

$$\frac{\partial}{\partial z}\{D(\psi)\{\frac{\partial \psi}{\partial z} - 1\}\} = \frac{\partial \psi}{\partial t} \tag{3.16}$$

To develop the one-dimensional θ-based Richard's equation we take the last term of equation 3.7.

$$\frac{\partial}{\partial z}\{K(\theta)\frac{\partial h}{\partial z}\} = \frac{\partial \theta}{\partial t} \tag{3.17}$$

Multiplying both sides by $\partial\theta/\partial\theta$ and recalling $h = \psi - z$, then

$$\frac{\partial}{\partial z}\{K(\theta)\frac{\partial(\psi - z)}{\partial z}\}\frac{\partial \theta}{\partial \theta} = \frac{\partial \theta}{\partial t} \tag{3.18}$$

$$\frac{\partial}{\partial z}\{K(\theta)(\frac{\partial\psi}{\partial z}-1)\}\frac{\partial\theta}{\partial\theta}=\frac{\partial\theta}{\partial t} \tag{3.19}$$

$$\frac{\partial}{\partial z}\frac{K(\theta)}{C(\theta)}\frac{\partial\theta}{\partial z}-\frac{\partial K(\theta)}{\partial\theta}\frac{\partial\theta}{\partial z}=\frac{\partial\theta}{\partial t} \tag{3.20}$$

$$+\frac{\partial}{\partial z}\{D(\theta)\frac{\partial\theta}{\partial z}\}-\frac{\partial K(\theta)}{\partial\theta}\frac{\partial\theta}{\partial z}=\frac{\partial\theta}{\partial t} \tag{3.21}$$

$$D(\theta)\frac{\partial\theta}{\partial z}-\frac{\partial}{\partial z}K(\theta)=\frac{\partial\theta}{\partial t} \tag{3.22}$$

This equation is similar to that derived by Yamada and Kobayashi (1988). They also pointed out the following empirical relationship, based on the fact that unsaturated hydraulic conductivity is a function of moisture content, where a and m are constants.

$$K(\theta)=a\theta^m \tag{3.23}$$

Richards' equations have hardly been used in modelling due to the complication in analytical solutions. What is more, the characteristic curve for each soil under consideration has to be known for the analytical solutions to be obtained. If a numerical approach is followed, a fair amount of computer time is required (Knight, 1983). Simple equations, most of them empirical, have been more popular in modelling. These include Horton, Philip and Kostiakov equations.

3.2 Factors Affecting Infiltration

Soil is a complex material, the characteristics of which vary in time and space. Soil infiltration characteristics are affected by many factors some of

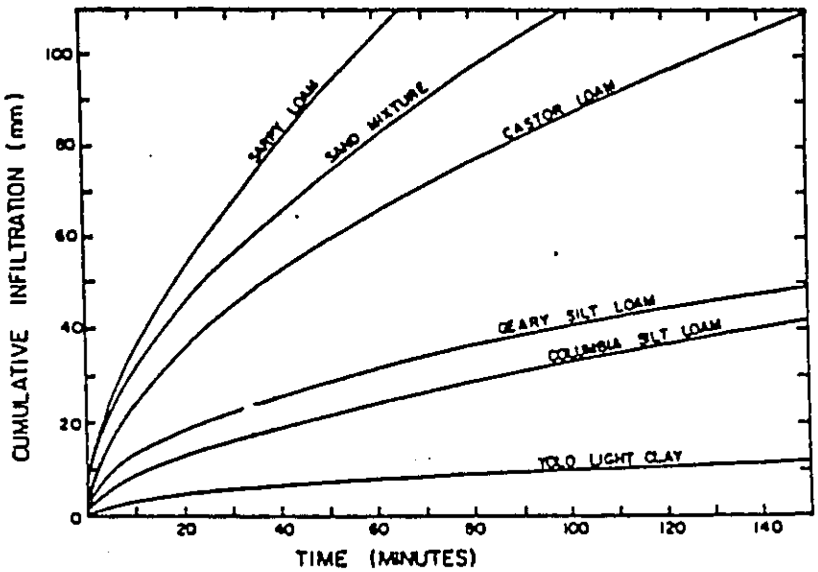

Figure 3.2: Variation of Infiltration with Soil Texture (after Skaggs and Miller, 1983)

which are briefly outlined below.

1. The rates of infiltration tends to be high in coarser soil texture. Figure 3.2 shows typical cumulative infiltration curves for soils of different texture. Infiltration not only depends on soil texture but also on soil structure. Hanks and Bower (1963) showed that variation in either diffusivity or soil water characteristics at water contents near saturation have very significant influence on infiltration predicted by means of Richards' equation. For this reason hydraulic soil properties should be measured accurately for water contents close to saturation, as far as infiltration is concerned (Skaggs and Miller, 1983).

2. Infiltration rates are higher for drier initial conditions. Figure 3.3 shows flux curves for infiltration, from a shallow ponded surface into a deep Columbia silt loam (Skaggs and Miller, 1983). Dependence

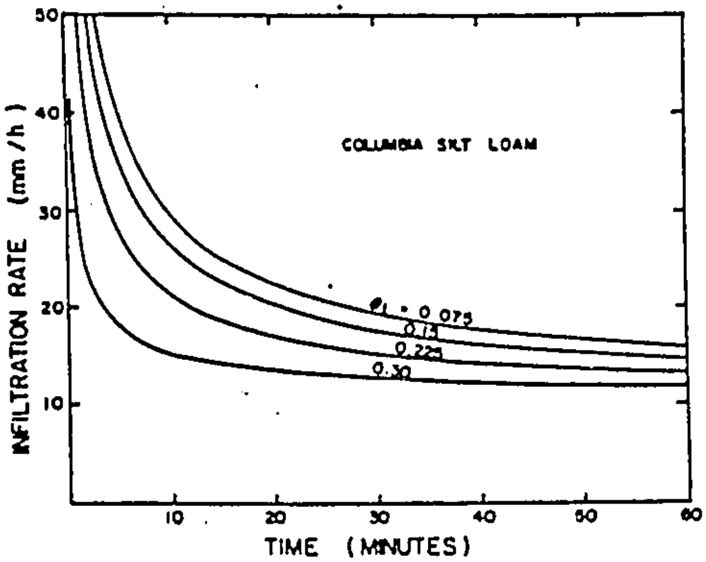

Figure 3.3: Dependence of Infiltration Rate on Initial Moisture Content (from Skaggs and Miller, 1983)

of infiltration on water content decreases with time. Infiltration rate should approach a constant value, usually equal to the saturated hydraulic conductivity K. Infiltration rates are higher at drier initial conditions because of the higher hydraulic gradients and more available storage volume.

3. Infiltration rates also depend on the application rate. For example should application rate be less than K, for a deep homogeneous soil, infiltration would continue indefinitely without ponding at the surface (Skaggs and Miller, 1983). Infiltration rate increases with water application rate. The time that surface ponding is initiated decreases with increasing water application rate.

4. The rate of water entry into the soil is affected by the conditions of the soil surface (Morel-Seytoux, 1983 and Thomas et al, 1981). Surface seals are formed under the influence of external forces such as rain drop impact, mechanical compaction or through slaking. Infil-

tration of water into bare soil can be markedly reduced by a seal-crust formed on the soil surface as a result of aggregate breakdown and compaction by the impact of raindrops (Ahuja and Rose, 1983). Morin and Benyamini (1977) concluded that the crust formed by rainfall impact is critical in influencing the infiltration capacity of a bare Hamra soil. To describe the infiltration process, three conditions (uncrusted dry soil, crusted wet soil and crusted dry soil) were considered. When simulated rainfall was applied at 130 mm/hr intensity, the infiltration capacity of bare Hamra soil decreased to 8 mm/hr in 60 minutes, as opposed to a continuous rate of 130 mm/hr when the surface was protected by a straw mulch. The soil crust can have a hydraulic conductivity as small as $\frac{1}{2000}$ of the hydraulic conductivity of the original soil. As a consequence the runoff and erosion are considerably increased (Thomas et al, 1981, Ahuja and Rose, 1983, and Eigel and Moore, 1983).

Water application on many freshly tilled soils causes gradual formation of a surface seal. The hydraulic conductivity of the seal decreases with time. A soil that has not been tilled after a previous rainfall may have a stable surface seal that does not increase following another rainfall event. One theory of the formation of surface seals is that soil aggregates are broken down then dispersed particles are washed into surface pores reducing their volume, then the surface is compacted by rain drop impact, producing a thin skin seal (Thomas et al, 1981).

5. As water infiltrates, the displacement of air is not complete. Since water application does not last long enough, full saturation of the pores is never attained. Where water flows, there remains some trapped immobile air at the so-called residual air content θ_{ar}. The air velocity V_a is close to zero. Air entrapment depends on soil pore geometry and on the capillary pressure of the soil. The presence of entrapped air causes additional reduction in infiltration. Since the pore space is

not fully saturated, the degree of saturation was referred to by Morel-Seytoux and Kanji (1974) as natural saturation or field saturation. The hydraulic conductivity at natural saturation $\bar{K}$ is less than the value at full saturation value, K.

Air can also be confined. In this condition, the air is at a pressure greater than atmospheric and it must either compress or escape. Residual air is entrapped at atmospheric pressure. Once ponding has taken place, compression is no longer negligible if air is confined. After a certain quantity of water has infiltrated, air will escape through the soil surface. The ponded surface will open to let air escape in a way to bring the confined air pressure to an equilibrium with the atmospheric air pressure. Just after the air escapes, the infiltration capacity jumps from a low value to a higher one.

6. Infiltration capacity is a function of both moisture content and hydraulic conductivity. The latter two soil properties are functions of suction head ψ. Figure 3.4 shows the variation of both $K(\theta)$ and θ with ψ. It also indicates that the relationships between ψ and θ and between ψ and K are hysteretic. At $\psi = 0$, the soil is saturated and $K(\theta) = K$ (hydraulic conductivity at saturation). Except for very simple initial and boundary conditions, and system boundaries, disregarding hysteresis, especially when air entrapment is a consideration, will lead to error in predicted water content, pressure distribution and surface fluxes (Kaluarachchi and Parker, 1987). These researchers suggest that when there is limited knowledge of hysteretic soil hydraulic properties. use of a simple parametric model for hysteresis will be preferred to disregarding hysteresis entirely.

   Since most hydraulic soil properties are dependent on soil physical properties. it is theoretically possible to predict some infiltration parameters such as K from the soil texture. However, Springer and Cundy (1987) found that texture-based procedure for estimating K

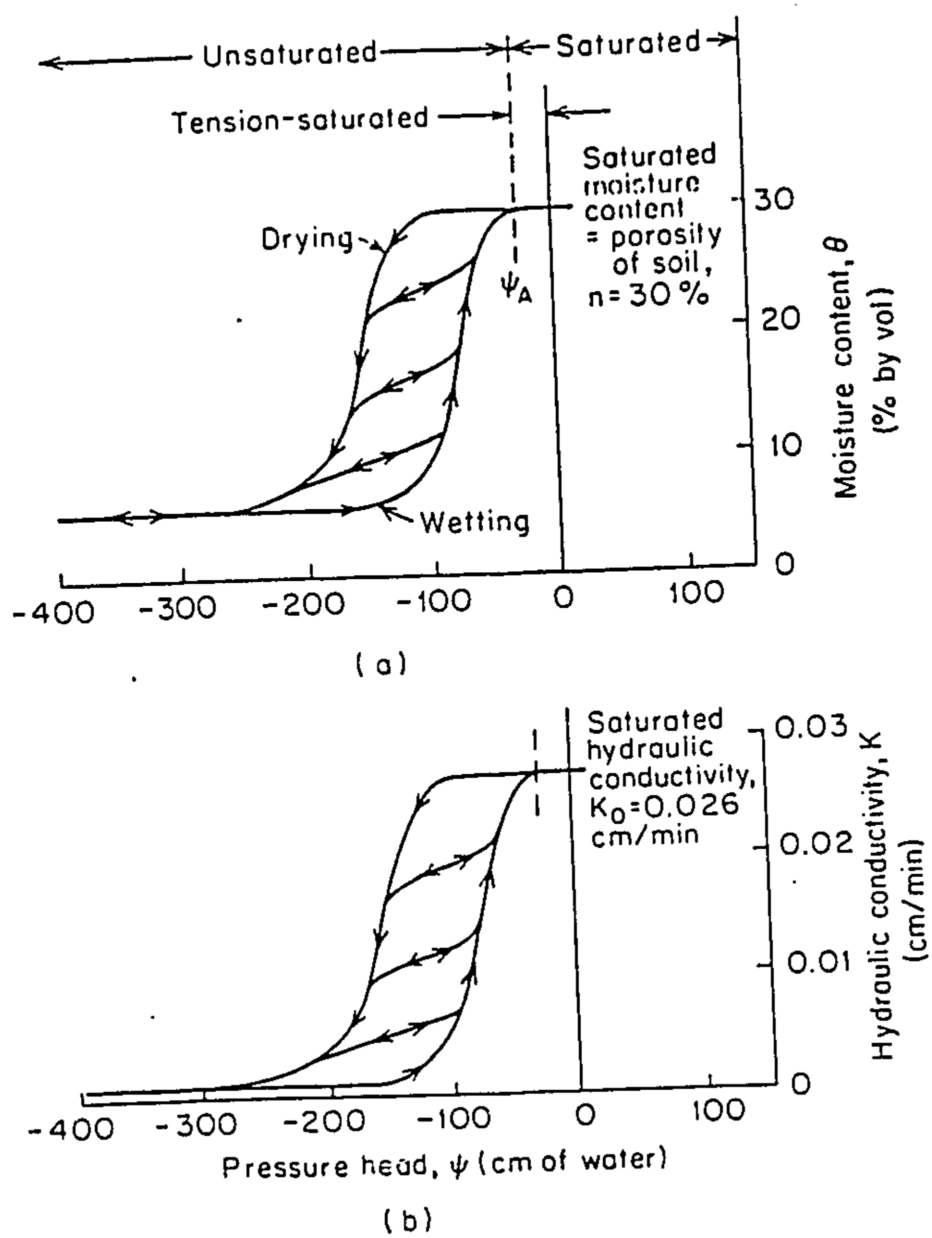

Figure 3.4: Hysteresis in Naturally Occurring Soils (After Freeze and Cherry, 1979)

performed poorly. So they concluded that hydrologic and soil physical properties are required for the determination of K.

3.3 Criterion of Efficiency for Predictive Models

In order to compare the various infiltration equations, a criterion of fitting efficiency must be established. Nash and Sutcliffe (1970) suggested such a criterion for assessing the fitting efficiency of rainfall-runoff models, based on the method of least squares. The fitting efficiency gives the proportion of observed sum of squares that is acc[illegible] for by the model. It has been adopted here to assess the fitting effici[illegible]tration prediction models.

If f represents the actual observed infiltration capacity at predetermined time steps, and f' is the corresponding infiltration capacity computed by the model, the residual sum of squares is defined by F_1:

$$F_1 = \sum^{n} i = 1(f_i - f_i')^2 \tag{3.24}$$

The initial sum of squares can be defined as F_0:

$$F_0 = \sum^{n} i = 1(f_i - f*)^2 \tag{3.25}$$

where f* is the arithmetic mean of the observed infiltration capacities.

$$f* = \frac{1}{n}\sum_{i=1}^{n} f \tag{3.26}$$

F_0 expresses the scatter associated with the crudest possible prediction, which is the arithmetic mean of the observed infiltration capacities. The efficiency of the predictive model (equation) is defined as:

$$E(\%) = \frac{F_0 - F_1}{F_0} \times 100 \tag{3.27}$$

This criterion of efficiency gives an indication of the goodness of fit and provides a basis for the comparison of different models. Where there is need to compare the effect of modifying an existing model, this criterion will give useful information. It gives a measure of the effectiveness of the modification.

One problem associated with this criterion is that it does not account for error made in the measurement of observed data.

3.4 Finite Difference Simulation of Discharge Velocity at Steady State

Often the basic infiltration rate of soil at saturated conditions is taken as an approximation of saturated hydraulic conductivity in field conditions. However, since the equipment used for the experiments (see chapter 4) was not necessarily representative of field conditions, particularly in the sense that there was an impervious barrier only 50 cm below the soil surface, the errors made in making this assumption may be high. Theoretical computations could help to determine the effect of an impervious barrier on infiltration rate at saturated conditions. The governing equation for steady state flow in homogeneous isotropic material is the Laplace equation:

$$\frac{\partial^2 h}{\partial x^2} + \frac{\partial^2 h}{\partial y^2} = 0 \qquad (3.28)$$

The derivation of the Laplace equation is similar to that of Richards' equation. It is a steady state flow equation. The law of conservation of mass requires that the rate of fluid mass flow into any elemental control volume (refer to Figure 3.1) be equal to the rate of fluid flow out of the element.

The continuity equation becomes,

$$-\frac{\partial(\rho V_x)}{\partial x}-\frac{\partial(\rho V_y)}{\partial y}-\frac{\partial(\rho V_z)}{\partial z}=0 \tag{3.29}$$

Assuming that the fluid is not compressible, the $\rho's$ can be eliminated from equation 3.29. The equation simplifies to

$$-\frac{\partial(V_x)}{\partial x}-\frac{\partial(V_y)}{\partial y}-\frac{\partial(V_z)}{\partial z}=0 \tag{3.30}$$

Substituting Darcy's law for the velocity terms it follows that

$$\frac{\partial}{\partial x}\{K_x\frac{\partial h}{\partial x}\}+\frac{\partial}{\partial y}\{K_y\frac{\partial h}{\partial y}\}+\frac{\partial}{\partial z}\{K_z\frac{\partial h}{\partial z}\}=0 \tag{3.31}$$

For an isotropic medium, $K_x = K_y = K_z$. If the medium is homogeneous the two-term form of Laplace equation becomes,

$$\frac{\partial}{\partial x}(\frac{\partial h}{\partial x})+\frac{\partial}{\partial y}(\frac{\partial h}{\partial y})=0 \tag{3.32}$$

The solution for h(x,y) at steady state allows the construction of a flow net describing the flow in a region with given boundary conditions. From the flow net the discharge and hence discharge velocity through a given system can be computed.

Finite difference simulation is one of the numerical methods that can be used to obtain the potential field and the flow net. It is based on the discretization of a continuum that makes up the region of flow. In the discretization, the area is divided into a finite number of blocks. Each block has a node at the center of which the hydraulic head is defined for the entire block. Figure 3.5 shows a typical arrangement of nodes.

Using Taylor expansion,

$$h_{i,j+1}=h_{i,j}+\frac{\partial h}{\partial y}\Delta y+\frac{\partial^2 h}{\partial y^2}\frac{(\Delta y)^2}{2!}+.... \tag{3.33}$$

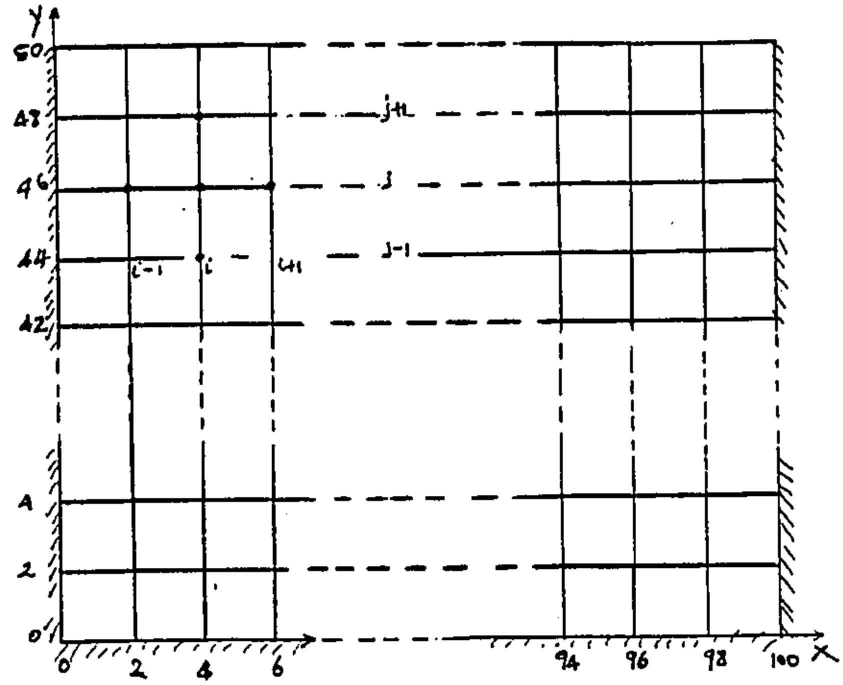

Figure 3.5: Nodal Grid for Finite Difference Flow-net Simulation

$$h_{i,j-1} = h_{i,j} - \frac{\partial h}{\partial y}\Delta y + \frac{\partial^2 h}{\partial y^2}\frac{(\Delta y)^2}{2!} - \ldots. \tag{3.34}$$

$$h_{i+1,j} = h_{i,j} + \frac{\partial h}{\partial x}\Delta x + \frac{\partial^2 h}{\partial x^2}\frac{(\Delta x)^2}{2!} + \frac{\partial^3 h}{\partial x^3}\frac{(\Delta x)^3}{3!} + \frac{\partial^4 h}{\partial x^4}\frac{(\Delta x)^4}{4!} + \ldots. \tag{3.35}$$

$$h_{i-1,j} = h_{i,j} - \frac{\partial h}{\partial x}\Delta x + \frac{\partial^2 h}{\partial x^2}\frac{(\Delta x)^2}{2!} - \frac{\partial^3 h}{\partial x^3}\frac{(\Delta x)^3}{3!} + \frac{\partial^4 h}{\partial x^4}\frac{(\Delta x)^4}{4!} - \ldots. \tag{3.36}$$

$$h_{i,j+1} + h_{i,j-1} = 2h_{i,j} + 2\frac{\partial^2 h}{\partial y^2}\frac{(\Delta y)^2}{2!} + O(\Delta x^4) \tag{3.37}$$

$$\frac{\partial^2 h}{\partial y^2} = \frac{h_{i,j+1} + h_{i,j-1} - 2h_{i,j}}{\Delta y^2} + O(\Delta x^4) \tag{3.38}$$

$$h_{i+1,j} + h_{i-1,j} = 2h_{i,j} + 2\frac{\partial^2 h}{\partial x^2}\frac{(\Delta x)^2}{2!} + O(\Delta x^4) \tag{3.39}$$

$$\frac{\partial^2 h}{\partial x^2} = \frac{h_{i+1,j} + h_{i-1,j} - 2h_{i,j}}{\Delta x^2} + O(\Delta x^4) \tag{3.40}$$

$$\frac{\partial^2 h}{\partial y^2} + \frac{\partial^2 h}{\partial x^2} = \frac{h_{i,j+1} + h_{i,j-1} + h_{i+1,j} + h_{i-1,j+1} - 4h_{i,j}}{\Delta x^2} = 0 \tag{3.41}$$

The approximation of hydraulic head $h_{i,j}$ at an interior point is given by;

$$h_{i,j} = 0.25(h_{i,j+1} + h_{i,j-1} + h_{i+1,j} + h_{i-1,j+1}) \tag{3.42}$$

The finite difference simulation assumes that $\Delta x = \Delta y$. The above equation states that, at steady state, the hydraulic head at any node in an isotropic material is the average of the four surrounding values. The finite difference (FD) equation for hydraulic head along the basal boundary, assuming the boundary to be impermeable, takes the following form (Freeze and Cherry 1979);

$$h_{i,j} = 0.25(h_{i-1,j} + h_{i+1,j} + 2h_{i,j+1}) \tag{3.43}$$

At a corner the equation becomes

$$h_{i,j} = 0.25(2h_{i-1,j} + 2h_{i,j+1}) \tag{3.44}$$

A finite difference equation is developed for each node in the grid. Repeated sweeps of calculation, top to bottom and left to right, through the nodal net is carried out. Each sweep is referred to as a relaxation. A starting value of h is assumed at each node. The most recently calculated value of h is always used at every node. Each pass through the system is called an iteration. After each iteration, the calculated h values approach the final answer more closely. The difference between the final and the current value of h is known as the residual, which decreases as the iterations proceed.

Once the flow net is complete, the flow through the system per unit length perpendicular to the flow net can be determined by construction of flow lines and equipotential. However, a more efficient method is to calculate the hydraulic gradient at each node, then calculate the respective discharge. Nodal discharge q is given by $q = Kia$ where K is the saturated hydraulic conductivity, a is the area of the block commanded by the respective node and i is the hydraulic gradient at the node. The total discharge through the system is the sum of the discharge through all the nodes in a straight line across the system and perpendicular to the direction of flow. Discharge velocity is obtained by dividing the total discharge by the total area.

From the finite difference simulations the average hydraulic gradients in various soil layers can be obtained. This enables the calculation of water discharge velocity through the layers.

Chapter 4

METHODOLOGY

Because the measurement of hydrologic data in the field always includes great uncertainty, a laboratory investigation was proposed in order to obtain more accurate measurement of all variables.

4.1 Apparatus and Experimental Set-up

Equipment already available in the hydraulics laboratory of the University of Ottawa was modified to enable the collection of tile flow, runoff and consequently infiltration data. An aluminium tank 2 m long, 1 m wide and 0.75 m deep was constructed and added as a modification to the existing equipment. A 2 m long 10 cm diameter tile drain was fixed at the bottom center of the tank. Its purpose was to collect percolating water from all over the soil box. The upstream end of the tile drain was closed while the downstream one was open. This ensured that the tile drain discharged at the downstream end of the soil box.

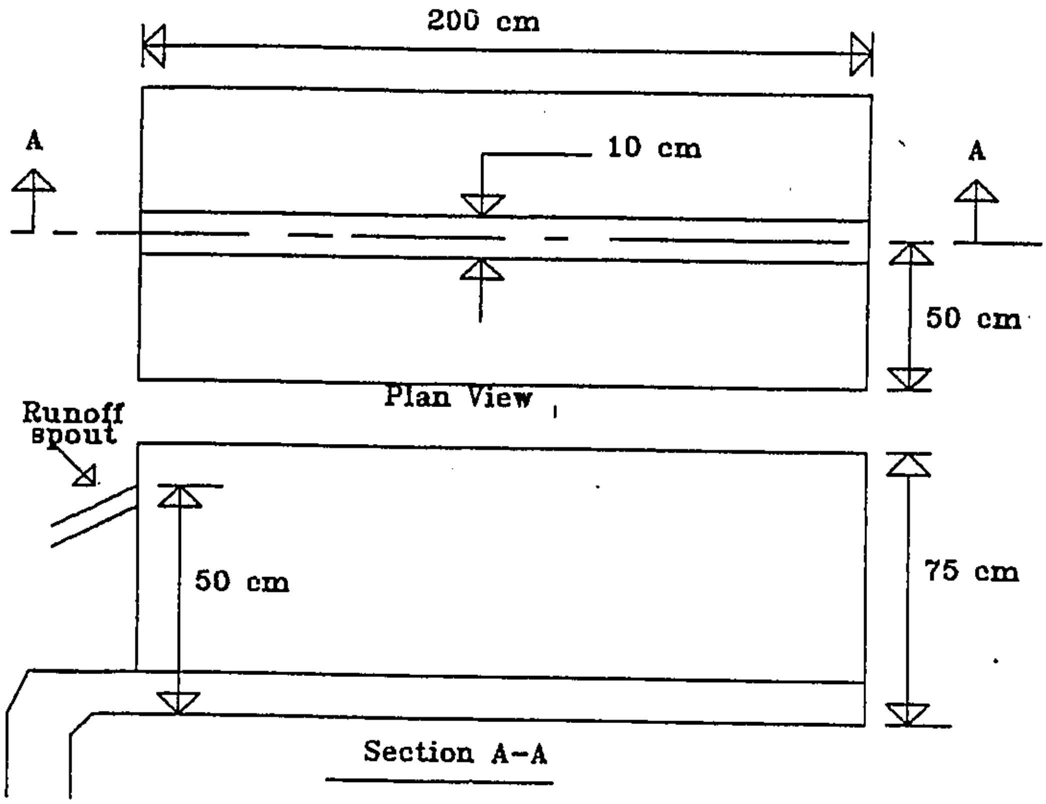

Figure 4.1: The Soil Box

An outlet spout was fixed 50 cm above the bottom of the soil tank. This enabled the measurement of runoff. Soil was packed into the box up to 50 cm from the tank bottom. A 2 cm clearance was left between the runoff spout and the soil.This ensured some ponding before runoff started. Soil packing was done in a way to ensure a 0.5% slope between the upstream and downstream ends of the soil bed.

The rainfall simulation system consisted of the following.
1. A water reservoir placed on the floor (see Figure 4.2).
2. A pump to lift water from the reservoir to a constant head water tank. Water was transmitted from the latter tank by gravity into the rainfall simulation nozzles.

3. An orifice to measure the rate of flow of water from the constant head tank. This had been calibrated to give flow in mm/hr.
4. A network of pipes bearing the rainfall simulation nozzles. These nozzles were simply 1 mm diameter holes drilled into the pipes. Nozzle spacing was 16.5 cm. Three pipes, each with 11 nozzles were used. The water spray produced by these nozzles was considerably different from naturally occurring rainfall. This is because the spray occurred as water jets and not droplets. However, it was felt that the precise simulation of rainfall type droplets was not essential to the purpose of the experiment. This was particularly because the soil was mainly sandy and so the sealing effect which would usually occur in soils of finer grain sizes would not occur in this case. With the help of a wire mesh screen, the water jets were broken into droplets.

4.2 Experimental Procedure and Measurements

A laboratory investigation was preferred because it would provide a more controlled environment. Macropore populations could be varied in a more precise and measurable pattern. Rainfall was simulated at a constant known rate which enables the computation of infiltration rate more precisely.

Soil used had to be permeable enough to allow water uptake and yet impermeable enough to allow runoff. The research was conducted in two parts. Experiment A was done with concrete sand modified with top soil. This choice was made since sand was readily available in the hydraulics laboratory. Both concrete and mortar sand were available. Their permeability was tested in the soil mechanics laboratory and concrete sand was found to

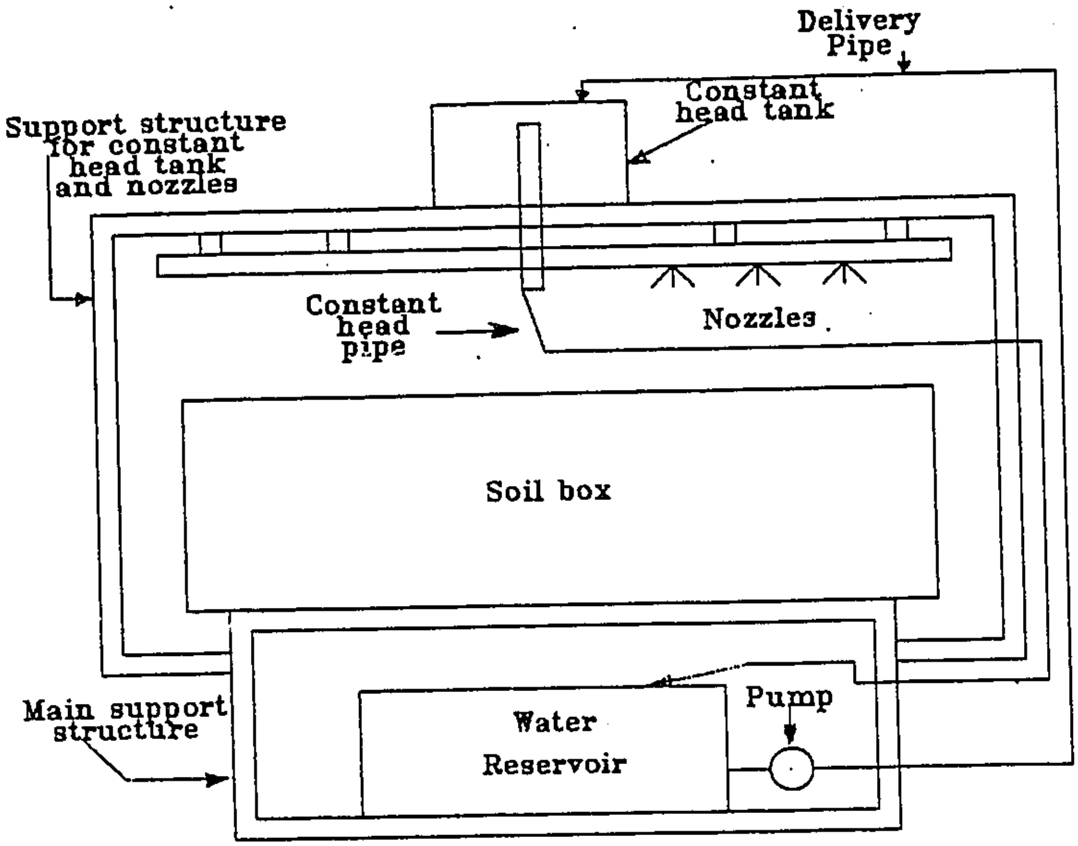

Figure 4.2: Rainfall Simulation Component

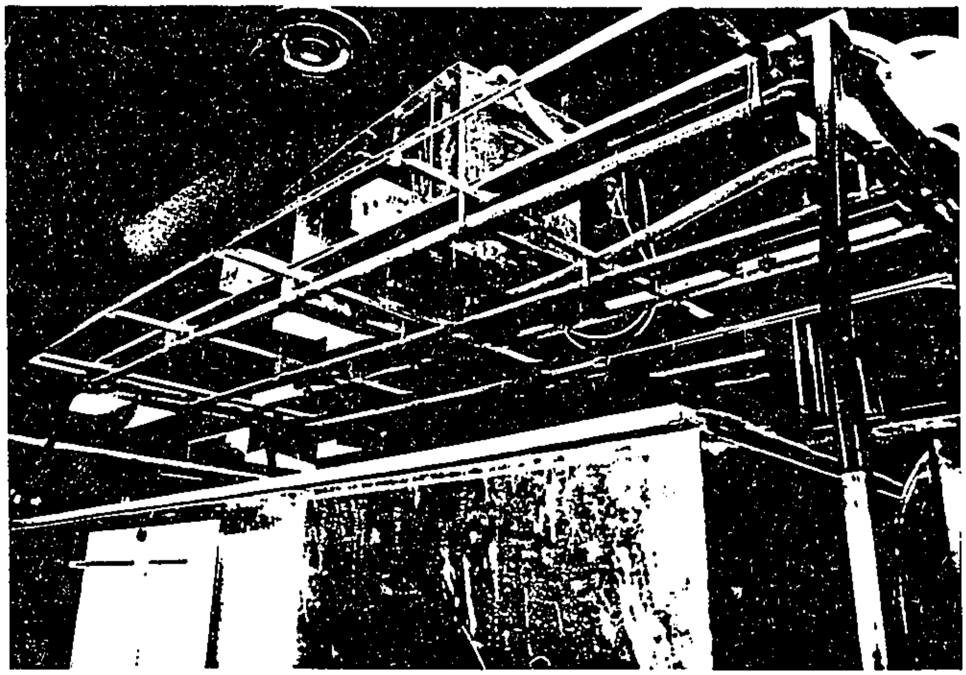

Figure 4.3: The experimental equipment (the overhead tank and soil tank)

have a lower permeability than mortar sand. This is because while mortar sand was highly uniform, concrete sand contained about 8 % fine material. The concrete sand was modified further by adding 25 % top soil, which was obtained from a flower gardening store. The blended soil was then found to have about 8 % clay, 6 % silt and 79 % sand. This qualified it to be called loamy sand. Its hydraulic conductivity was found to be about 35 mm/hr. In experiment 1 the whole 50 cm available for soil was filled with loamy sand.

Using soil with a high content of sand was desirable in case there was need to disturb the soil. Since sand is not exceedingly cohesive, it is more likely to maintain the same aggregate arrangement and possibly bulk density after unavoidable soil disturbance. Sandy soils tend to be more workable than most other soils. Less permeable naturally occurring soil was used for experiment B which was done with 45 cm of loamy sand covered with a 5 cm layer of sandy clay loam with gravel, which had about 30 % clay, 20 % silt, and 40 % sand. Its hydraulic conductivity was about 14 mm/hr. Figure 4.3 and 4.4 show the particle size distribution of the two soils. These curves were determined using the usual sieve and hydrometer methods of analysis.

The rainfall intensity used had to be high enough to produce runoff in the more permeable loamy sand even with the presence of macropores. That is why an intensity of 60 mm/hr was chosen.

Before any measurements were done, the soil was well packed in the tank by rolling a 5 kg concrete block on the soil after it had been poured into the box. A final gradient of 0.5 % was obtained. The downstream end of the soil bed was 0.5 cm lower in elevation than the upstream end. It was important not to disturb the soil unnecessarily during the experiments, since this would influence soil water intake capacity. The dry bulk densities of loamy

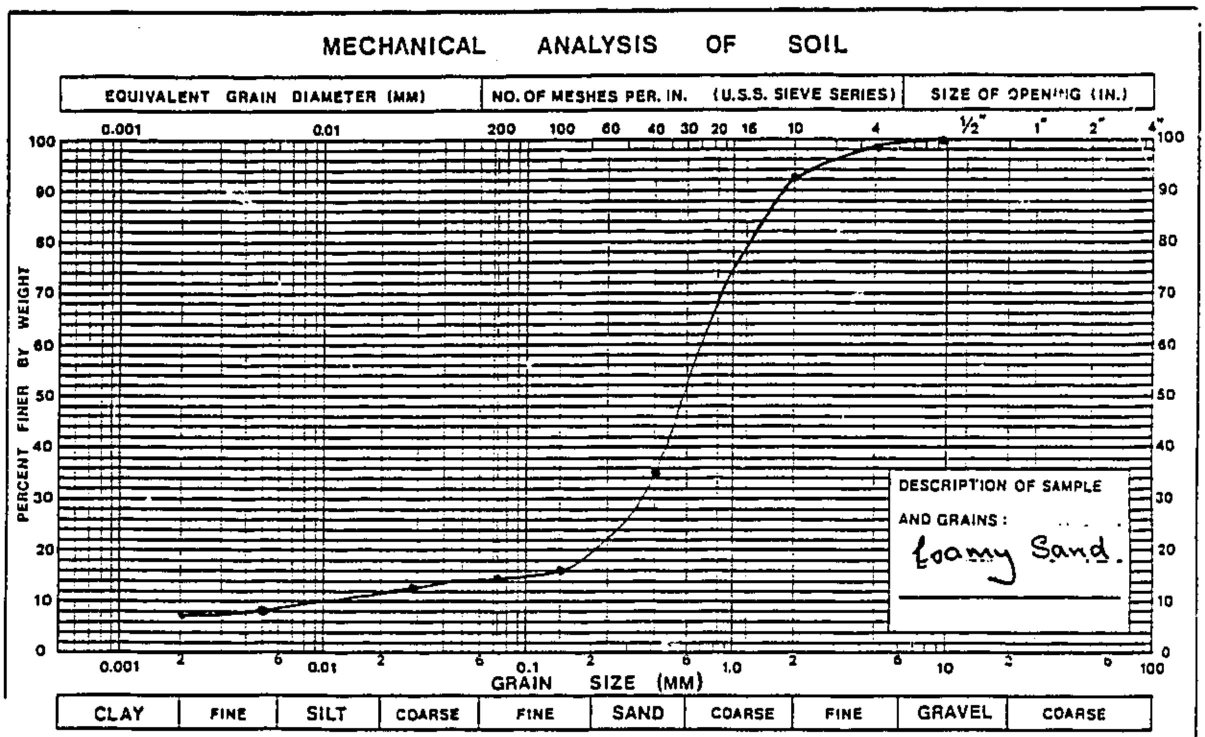

Figure 4.4: Particle Size Distribution-Loamy Sand. Exp. A

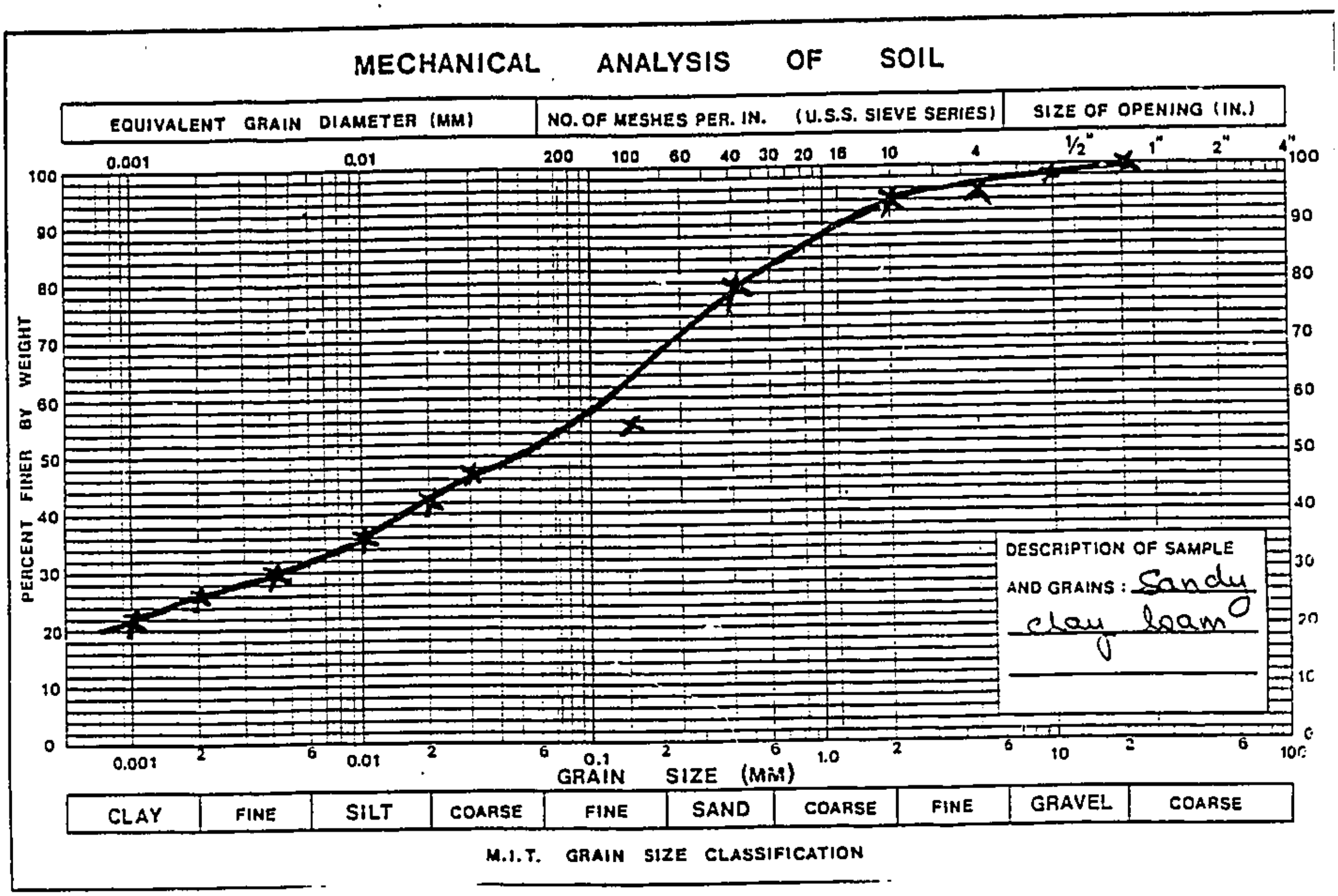

Figure 4.5: Particle Size Distribution-Sandy Clay Loam, Exp. B

sand soil and the sandy clay loam as they were during the experiments were found to be 1150 kg/m^3 and 1350 kg/m^3 respectively.

4.2.1 Macropore installation

Macropores were made in the soil by simply drilling 10 cm deep holes into the soil by means of a 1 cm diameter metallic rod. In experiments A and B, the number of macropores was increased from 0 to 24 uniformly. It was not convenient to reverse from a large number of macropores to a smaller number, since this would involve disturbing the soil and there was no guarantee that the soil condition after the disturbance would be the same as before.

In experiment A macropore numbers were increased by an increment of 4, in experiment B the increment was 2. Figures 4.5 and 4.6 show that the first macropores were put at the centre of the box and that extra macropores were put on both sides of the centerline such that macropores spread from the center of the tank with time. This attempted to make each increment in macropores have the same effect on soil water uptake. The numbers in figures 4.5 and 4.6 show the order in which the macropore were installed. The downstream portion of the bed was lower than the upstream and so there was a tendency for ponding to take place. In steady conditions, about 80 % of the whole bed surface was ponded. The runoff outlet was placed about 0.5 cm above the soil surface at the downstream end of the box. Macropore contribution to soil water uptake is greatly influenced by ponding. Macropores were eroded by unbroken water jets, particularly in the more loose soil. This changed the influence a macropore had on soil water uptake as time went by. Erosion on older macropores was less in experiment B since the soil used was more cohesive and therefore less erodible. To further reduce erosion, kinetic energy of the water was dissipated by placing stones at the positions of water jet impact.

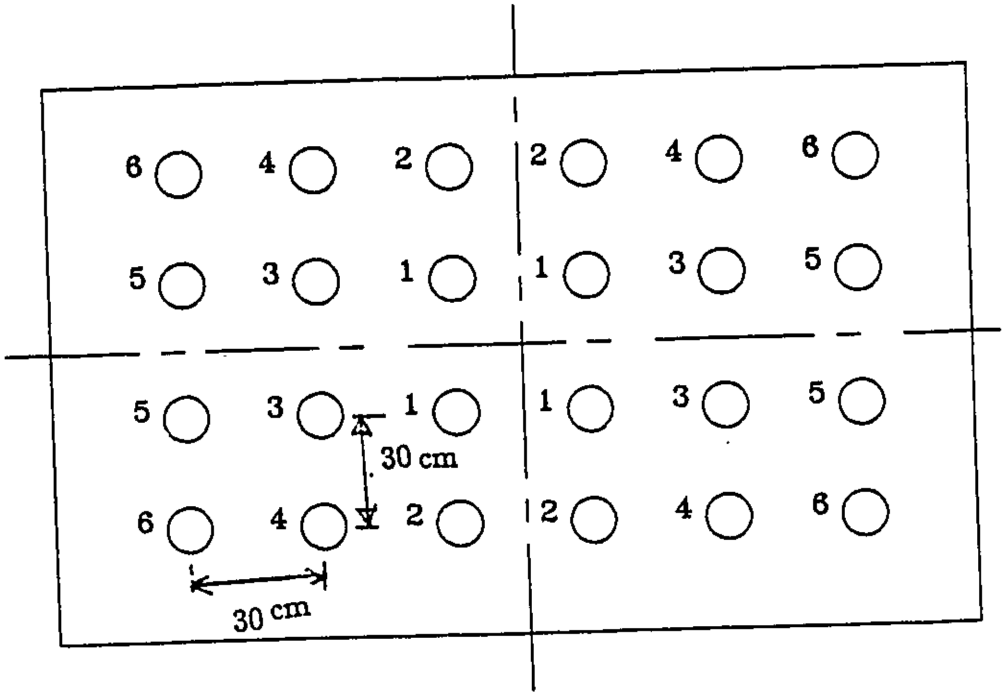

Figure 4.6: Installation of Macropores-Experiment A

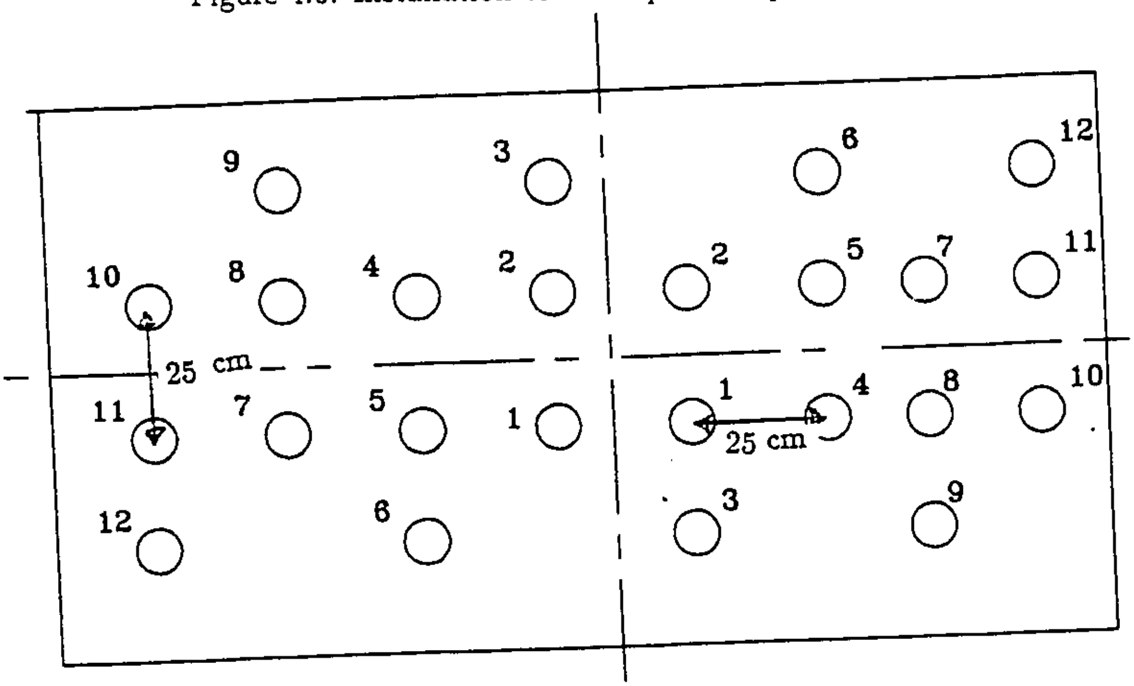

Figure 4.7: Installation of Macropores-Experiment B

4.2.2 Measurement

Runoff was measured directly by collecting flow from the runoff outlet in the soil box. At the beginning, when runoff rate was low, a 500 ml measuring cylinder was use to catch the flow. A stop watch was used for timing, and the volume of runoff collected in 30 seconds was recorded. When runoff rate increased, such that the volume of runoff obtained in 30 seconds was more than 500 ml, a larger container of capacity 5 litres was used to catch runoff. Runoff rate was measured about once every 2 minutes at the beginning, when the rate changed very rapidly. Later, readings were taken once every 5 to 10 minutes. In a similar way, tile flow was measured. After every rainfall event, some outlets at the bottom of the soil box were opened. This made it easier for the soil to drain. Each time the soil was given 36 hr. to drain. The moisture content after that time was about 26 %. Field capacity, which is the moisture content after about 24 hr, was about 27 %. Maintaining the drying period the same ensured that soil moisture content at the beginning of each rainfall event was essentially the same

It was necessary to ensure that there was sufficient water in the reservoir to avoid running the pump dry in the event of the reservoir running dry during the experiment.

An experimental run started with the outlets at the bottom of the soil tank closed. The selected number of macropores was drilled and rainfall simulation set on. Water was pumped into the overhead tank until overflow started. The inlet to the rainfall simulation nozzles was opened and the relevant valve adjusted to give rainfall intensity of 60 mm/hr. From the start of the rainfall, it took about 10 minutes for runoff to start. This could be called ponding time.

4.3 Processing of experimental data

The runoff and tile flow were measured in ml/30s. Knowing that the area of the soil bed was $2m^2$, the latter units were changed into mm/hr. Observed infiltration was calculated as the difference between a rainfall intensity of $60mm/hr$ and runoff (mm/hr). All the processing was done with the help of the a LOTUS 123 spreadsheet. Observed cumulative runoff, infiltration and tile flow were calculated by the "summation method". For example cumulative (total) infiltration at time t_i, denoted by F_i, is given by the equation,

$$F_i = (t_i - t_{i-1})(f_i + f_{i-1})/2 + F_{i-1} \tag{4.1}$$

The symbol f_i represents infiltration capacity at time t_i; the above way of computation is referred to as the summation method. The total infiltration (F) during the one hour rainfall is computed for $t_i = 1$ hour. Runoff and tile flow are treated similarly.

Not much is known about the infiltration capacity of the soil between starting time of the rainfall and the first time runoff is observed. If the time runoff starts is denoted by t_0, it can be said that the infiltration capacity between start of rainfall and time t_0 is at least equal to the infiltration capacity at t_0. Let the latter infiltration capacity be denoted by f'_0. The total infiltrated volume at time t_0 is approximated as $t_0 \times f'_0$.

If $t_0 = 0.13\,hr.$ and $f'_0 = 55.6\,mm/hr.$,
then $F_0 = 0.13 \times 55.6 = 7.2$ mm/hr With the experimental data thus processed, it was possible to undertake the comparison of the infiltration equations.

It is noted that in nature macropores are more complex than what was simulated in the laboratory study. However, since the installation of the large pores provided paths of less resistance for infiltrating water, this produced a macropore effect the evidence of which is given in the result and the discussions.

Chapter 5

ANALYSIS

5.1 Fitting Infiltration Equations to Experimental Data.

The three infiltration equations fitted to the experimental data were Horton, Philip, and Kostiakov equations.

Horton equation, given by equation 2.1, can also be linearized by writing

$$ln(f - f_c) = ln(f_0 - f_c) - kt$$

With the help of the regression analysis package of LOTUS. 123 software, $ln(f - f_c)$ was fitted as a function of t. The x-coefficient given by the regression analysis was equated to -k while the y-intercept was equated to $ln(f_0 - f_c)$, from which parameter f_0 could be computed. Figure 5.1 shows an example of a LOTUS spreadsheet. The regression coefficient R^2 was one of the parameters used to give a measure of goodness of fit. The other parameter was fitting efficiency ($E\%$) discussed in chapter 3.

0 Macropores

Infiltration Data

	Time (Hr.)		Observed Infilt. (mm/hr)	(f-f*)^2	F (mm)	ln(f-fc)	Horton (Simulated) (mm/hr)	(f-f')^2
	0.00					ERR		0.00
	0.13		55.60	579.9	7.51	3.80	40.0	243.59
	0.15	A	50.8	371.8	8.58	3.68	37.6	174.00
	0.17		45.90	206.8	9.55	3.55	35.4	109.80
	0.18		42.0	109.9	9.98	3.43	34.4	57.82
fc=	0.22		32.40	0.8	11.47	3.06	30.7	2.87
11.00	0.23		30.00	2.3	11.78	2.94	29.9	0.01
	0.25		24.0	56.5	12.32	2.56	28.3	18.73
	0.27		21.0	110.6	12.77	2.30	26.9	34.84
	0.28		18.0	182.7	12.97	1.95	26.2	67.82
	0.50		15.0	272.9	16.60	1.39	16.9	3.72
	1.00		12.0	381.0	23.35	0.00	11.7	0.09

fc= 11.00

f*= 32

sum(f-f*)^2 = 2275.22

sum(f-f')^2 = 713.30

E = 68.6 %

HORTON EQUATION

Regression Output:

ln(fo-fc)	Constant		3.93
50.6	Std Err of Y Est		0.44
	R Squared		0.87
fo=	No. of Observations		11.00
61.6	Degrees of Freedom		9.00
k=	X Coefficient(s)	-4.29	
4.29	Std Err of Coef.	0.56	

Figure 5.1: Fitting Horton Equation to Experimental Infiltration Data, Expt B (LOTUS 123 Spreadsheet)

Parameter f_c was assumed to be equal to the least observed infiltration capacity less 1 mm/hr. This is done because theoretically f_c can only be reached at time infinity, yet infiltration was only allowed to continue for 60 minutes. It is also important for f_c to be less than all the observed values of f, since a real value of $ln(f - f_c)$ only exists when the difference between f and f_c is greater than zero. For example in the case of experiment B, the least observed infiltration capacity was 12 mm/hr, and thus $f_c =$ 11 mm/hr. Depending on the appearance of the infiltration curve, a small number like 0.1 mm/hr would be subtracted. This would be the point where the infiltration capacity curve looks almost horizontal.

As indicated in equation 2.7, Philip Equation is written as

$$f = 0.5St^{-1/2} + A.$$

Infiltration capacity f and $t^{-1/2}$ are linearly related. Regression analysis of $t^{-1/2}$ as the X-axis data and f as the Y-axis data was done. The x-coefficient was equated to 0.5S while the y-intercept (or constant) was equated to parameter A.

Kostiakov Equation, as presented in equation 2.5 , does not present a linear relationship between f and t. However, the equation can also be written as

$$lnf = lnA + Blnt.$$

Treating $ln\,t$ as X-axis data and $ln\,f$ as Y-axis data, regression analysis produce x-coefficient equal to B and Y-intercept equal to $ln\,A$. Parameter A could then be computed.

The calculation of cumulative infiltration was done by plugging in parameter values into the cumulative infiltration form of the various equations. If the total observed infiltration is denoted by F and the total infiltration computed from the equation data is denoted by F_s, then the error made in prediction of total infiltration is given as

$$\frac{F - F_s}{F} \times 100 \tag{5.1}$$

5.2 Finite Difference (FD) Simulation of Discharge Velocities

A finite difference scheme is essentially a number of nodes covering the area of interest. It is usually described by means of square grids. A section 100 cm wide and 50 cm deep was studied. Equations 3.42 to 3.44 give expressions for the hydraulic heads at an interior node, a node on the basal boundary and one at a corner, respectively. Figure 5.2 shows nodes in the three locations.

From the experimental data it was found that the ratio between final infiltration capacity in the less pervious to the more pervious layers was 11:26 respectively. This can be rounded off to an equivalent of 1:2.5. This was taken to be the ratio of the values of saturated hydraulic conductivity in the two layers. When there are layers of soil with different permeabilities, the procedure suggested by Cedergren (1977) was used to make the analysis possible. His method, illustrated in Figure 5.2, suggests that in the less permeable medium, equipotential lines must be squeezed together, while in the more permeable layer they are further apart. This ensures a greater drop in potential in the less pervious medium. The ratio of equipotential densities depends on the ratio of hydraulic conductivities, K_2/K_1, where $K_2 > K_1$.

Since $\frac{K_2}{K_1} = 2.5$, the nodal densities used were 1 node per centimeter in the less permeable layer and a density of 1 node per 2.5 cm in the more

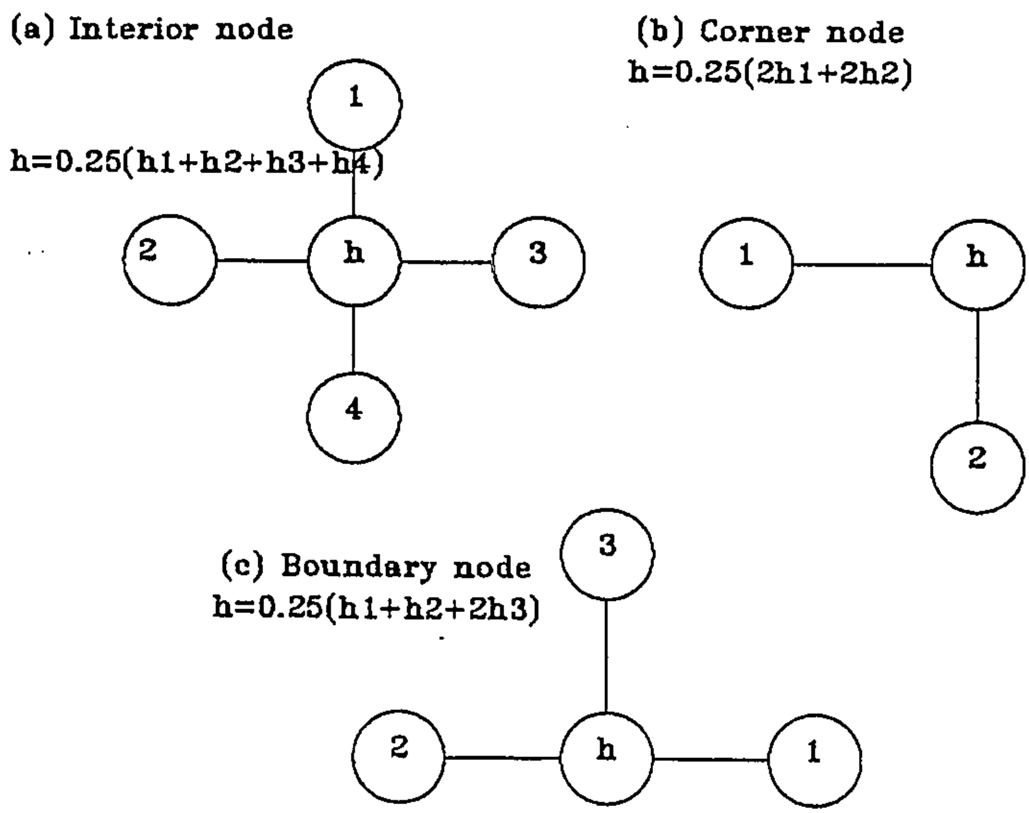

Figure 5.2: Interior, Corner and basal boundary nodes

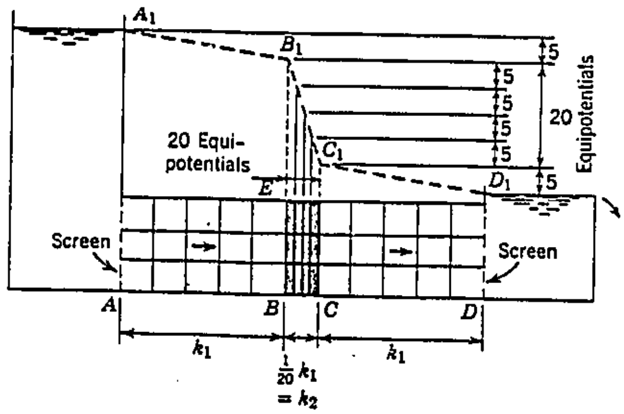

Figure 5.3: A Simple Two-Permeability Flow Net (after Cedergren 1977)

permeable layer.

In case of 2 layers, the thicknesses of the more permeable and the less permeable layers are 45 and 5 cm. respectively. The total depth of the uniform porous material is 50 cm.

$$q_{i,j} = K \frac{dh}{dx}_{i,j} \tag{5.2}$$

Quantities $q_{i,j}$ and $\frac{dh}{dx}_{i,j}$ are specific discharge and hydraulic conductivity at node (i,j) (see Figure 3.6). For a given value of j, i lies between 1 and n, where n is the total number of nodes along the width of the section. The total discharge through the section, per unit length perpendicular to the section, is given by;

$$Q = \sum_{i=1}^{n} q_{i,j} . a_{i,j} \tag{5.3}$$

The area influenced by node (i,j) is denoted by $a_{i,j}$. If all nodes command equal areas, then area 'a' per unit length perpendicular to the section is given by

$$a = \frac{L}{n} \times 1 \tag{5.4}$$

L = the width of the section. The average discharge velocity (V) equals discharge per unit area:

$$V = Q/(L \times 1) = \frac{1}{L} \sum_{j=1}^{n} q_j . \frac{L}{n} \tag{5.5}$$

The results of the analysis of experimental data are presented and discussed in the next chapter. As well, findings from the finite difference simulations are given in the same chapter.

Chapter 6

RESULTS AND DISCUSSION

In this chapter, the results from the analyzed laboratory data and the findings from the finite difference simulations are presented and discussed. Tests done in homogeneous sandy soil (experiment A) produced data A, while the non-homogeneous case (experiment B) produced data B. In both experiments, the effect of increasing the number of macropores on infiltration and percolation patterns was investigated. In the homogeneous soil test there was a 50 cm deep sandy soil profile. In experiment B, the lower 45 cm was a layer of relatively permeable sand. This was covered with a 5 cm relatively less permeable clay soil layer.

As can be seen in Figure 6.1, the appearance of experiment A infiltration curves was different from experiment B infiltration curves. In the case of data A, the infiltration rates lowered with time until a certain minimum was reached, then there was a slight increase. This phenomenon, which was also noted by Morel-Seytoux and Khanji (1974), is associated with the presence of entrapped gases. The slight increase in infiltration rate is thought to take place as entrapped gases escape. When air movement stops, equilibrium

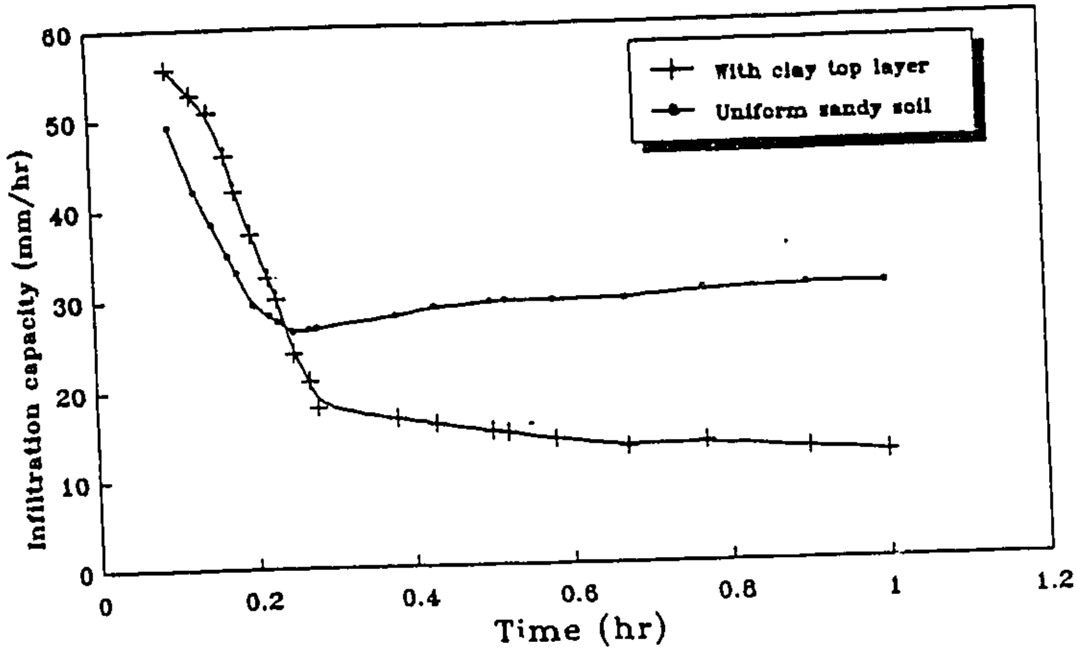

Figure 6.1: Experimental Infiltration Rates

infiltration capacity is attained. This phenomenon usually happens where an impermeable horizontal boundary exists not too far from the water table.

Some possible reasons why the above phenomenon was noticed only in the homogeneous more permeable soil are that:

1. The more pervious soil has large pores which permit fast movement of water into the soil and hence entrap some gases within the soil.
2. Since there are large pores in the sandy soil. it is easy for gases to find a way of escape. Trapped air effect is only noticed after the entrapped air escapes.
3. The clay layer in the non-homogeneous soil profile will allow water uptake at relatively slower rate. This could mean that less air is entrapped.
4. Since the clay layer has a surface sealing effect, it is not very easy for entrapped air to escape. As it has been mentioned above the effect entrapped air cannot be seen unless some air escapes. reducing the resistance against water movement at the infiltration front.

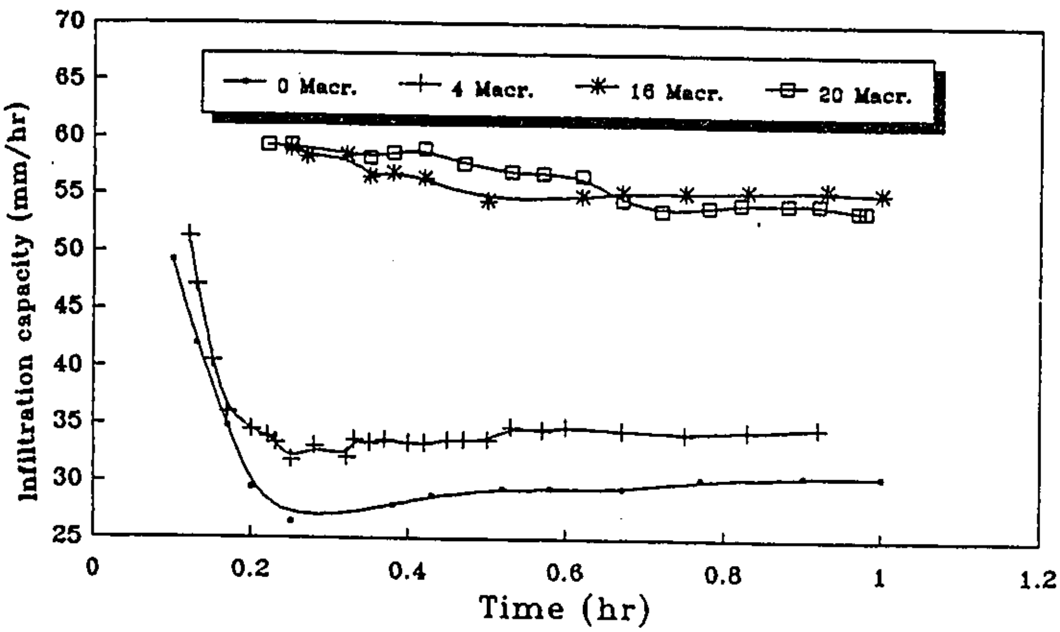

Figure 6.2: Effect of Macropores on Basic Infiltration Rate

6.1 Macropore Index Concept

All infiltration parameters were found to change with changing macropore populations. Figure 6.2 shows that increasing numbers of macropores in the soil generally tends to increase the basic infiltration capacity (f_c). The maximum value f_c can attain is the rainfall intensity. In experiment A, going beyond 16 macropores produced negligible effect on infiltration capacity (see Figure 6.3). It can even be seen that in some cases infiltration curves may intersect. This is associated with experimental error.

The effect of increasing macropore populations on other infiltration parameters is discussed further on in this chapter. Describing the effect of macropores in terms of number of holes drilled into the soil is not a very efficient method. Some researchers have attempted to quantify macroporosity in terms of the volume of gravity water contained in a unit volume of soil

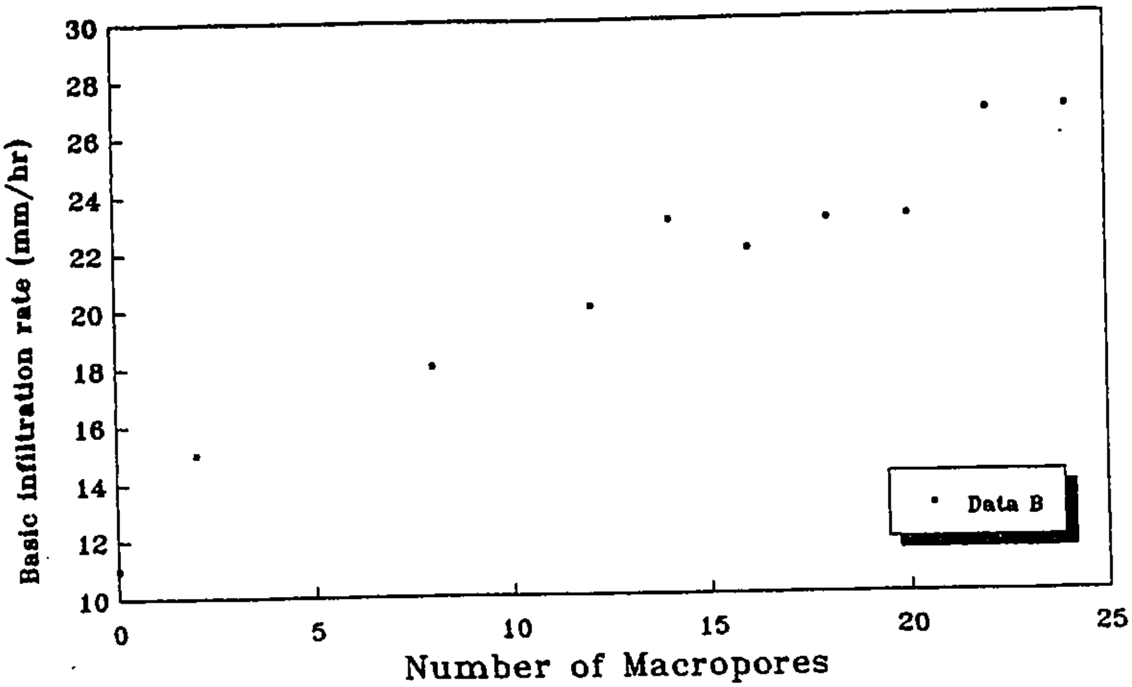

Figure 6.3: Effect of Macropores on Infiltration Rate

(Nelson and Gregory, 1988). In this thesis a new tool, macropore index, is introduced. The concept attempts to give a measure of the population of non-capillary pores without having to talk in terms of numbers or volume.

The largest observed value of f_c is denoted by f_{c0} while the corresponding value of N is denoted by N_0. In this case N_0 is 24 (see Figure 6.2). An index, n, of macroporosity could be obtained by dividing number of macropores used by N_0.

$$n = \frac{N}{N_0} \tag{6.1}$$

Doing this produces an index which ranges between 0 and 1. Change in parameters of infiltration can now be described in terms of the index. For example Figure 6.4 shows the variation of f_c with n.

The fact that a curve describing the change of f_c with n can be produced makes it possible to use changes in f_c as an indicator of changes in

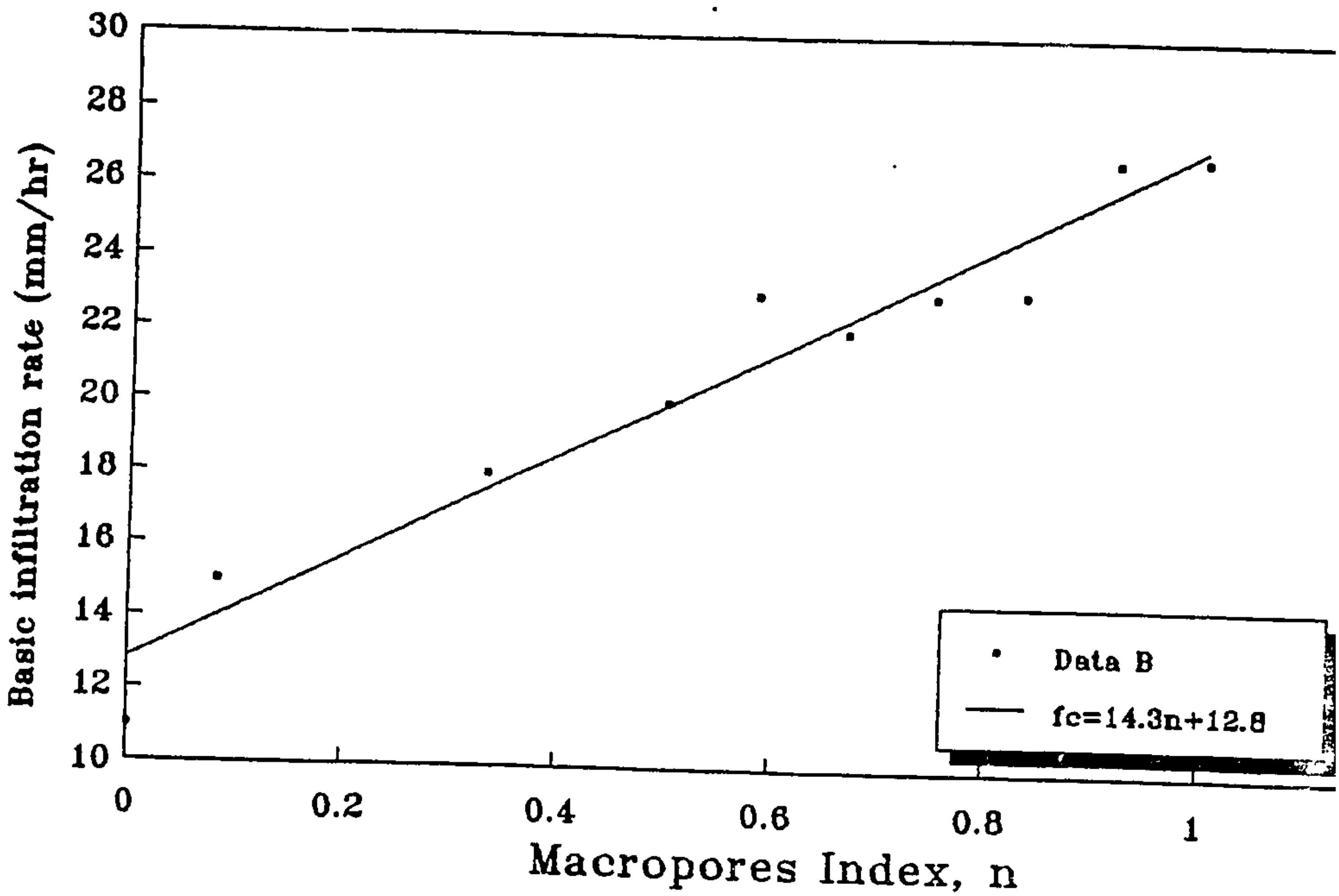

Figure 6.4: Change of Basic Infiltration Capacity with Macropore Index (M-Index)

macropore index (M-index). The index can be read off the curve as long as the f_c is known. In practice M-index is expected to change at a particular location perhaps seasonally. It is possible to allocate values M-index for the different seasons of the year. The accuracy in allocating values of M-index would depend on experience. Perhaps this could be done in a way similar to the SCS method of allocating CN values.

If it is assumed that f_c is equal to the soil saturated hydraulic conductivity, K, then the variation of K with changing number of non-capillary pores can be described using a macropore index. Describing the variation of infiltration equation parameters in terms of this index is more useful than using the number of macropores N.

The following section shows how a finite difference simulation of water flow into porous material was used to study the effect of macropores on steady state discharge velocity. The effect of an impervious barrier close to the soil surface has also been investigated using this simulation method.

6.2 Finite Difference (FD) Simulation of Discharge Velocities

Finite difference simulation of discharge velocities at steady state was carried out in order to study numerically how variation of macroporosity affects the rate of flow of water into the soil. The volume of water infiltrating the soil per unit time is referred to as discharge while the discharge per unit area is called discharge velocity. Increasing discharge velocity at steady state gives the impression that the soil has attained a higher hydraulic conductivity. This may often not be the case. The presence of macropores does not affect the soil matrix. Hydraulic conductivity is a function of soil grain size and the chemical composition of the soil. So it may be more accurate to say that macropores influence the 'apparent saturated hydraulic conductivity' of the soil.

In the computations (explained in chapter 5), it is assumed that hydraulic head depends solely on vertical elevation. The presence of an impermeable bottom boundary and tile drain interfere with the hydraulic heads such that this is no longer true. Also the presence of two layers complicates matters further. To make the study convenient, four cases were considered.

Case 1:

In this case simulations were done for homogeneous soil. Square grids of 2 cm length were adopted (see Figure 5.1). Impermeable bottom boundary and tile drain were assumed to be absent. Hydraulic heads of 50 cm and 0 cm were assumed at the soil surface and at the bottom of the tank, respectively. This simulation gives us the hydraulic gradients we would expect if there was neither bottom impermeable boundary nor tile drain. In the absence of macropores, the hydraulic gradient is unity.

Case 2:

This was the same as case 1 only that the bottom impermeable boundary and tile drain were considered present. The hydraulic gradients in the absence of macropores no longer depended on vertical elevation alone. For N = 0, the hydraulic gradient was found to be 0.74. To indicate the 10 cm diameter tile drain a hydraulic head of 0 cm was fixed in a circle 10 cm in diameter on the centerline at the bottom of the tank. It was not possible to produce a circular shape. A square shape with cut corners was used to approximate a circular shape.

Case 3:

A two-layer soil profile was considered. Horizontal distance of 5 cm between nodes was adopted. This made it possible to have 5 nodes per 5 cm in the vertical direction, in the less permeable layer, while in the more permeable,

Table 6.1: Average Hydraulic Gradients

N	Case 1	Case 2
0	1.00	0.74
4	1.06	0.76
8	1.11	0.80
12	1.17	0.83
16	1.20	0.84
20	1.23	0.86
24	1.29	0.863

there was 1 node per 5 cm in the vertical direction. A hydraulic head of 50 cm was fixed at the soil surface while a hydraulic head of 27 cm was put at the bottom of the tank. This made it possible to obtain a hydraulic gradient of unity in the less permeable material, for N = 0.
Case 4:
This was the same as case 3 but this time an impermeable bottom boundary and a tile drain were considered. As in case 2, the tile drain was indicated by fixing the lowest hydraulic head in the tile drain. In this case, in order to be consistent with case 3, the lowest hydraulic head was 36 cm. For N = 0, the hydraulic gradient was 0.77.

Since in the cases of two-layer soil profile fewer nodes were used, larger macropores than in the case of homogeneous soil had to be considered. In the homogeneous material it was possible to simulate macropores with as small as 2 cm diameters, but with fewer nodes in the non-homogeneous case, the minimum possible macropore diameter was 5 cm.

Tables 6.1 and 6.2 show that for soil without macropores, the presence of a bottom impermeable layer and a tile drain in homogeneous soil reduces

Table 6.2: Average Hydraulic Gradients

N	Case 3	Case 4
0	1.00	0.77
2	1.06	0.85
4	1.11	0.91
6	1.17	0.94
8	1.20	0.96
10	1.23	0.97

the hydraulic gradient to 74 % of the original value. Also, in the two layer soil profile, the impermeable bottom boundary and the tile drain cause a reduction to 77 % of the initial value.

At steady state, Darcy's law is

$$V = f_c = Ki$$

where f_c is final infiltration rate, which is the vertical movement of water from the soil surface into the soil matrix at steady state. Discharge velocity (V), or steady state infiltration rate, is proportional to hydraulic gradient. Writers and researchers in the subject of infiltration always state that saturated hydraulic conductivity K can be taken approximately equal to the equilibrium infiltration capacity (Skaggs, 1983). However the conditions in which the assumption that $K = f_c$ is valid are seldom specified.

The quantity V will only be equal to K when the hydraulic gradient equals unity. In such a situation hydraulic gradient would depend only on the vertical elevation of the point under consideration. This would be the case when there are no restricting impermeable boundaries. It is then required that the soil profile be deep and unbounded on the sides.

Table 6.3: Change of Basic infiltration capacity with N, Data A

N	0	4	8	12	16	20	24
f_c	26	31	35	48	53	54	55

From table 6.3, the discharge velocity, or equilibrium infiltration capacity in the absence of macropores, in experiment A was 26 mm/hr. Considering the FD simulation, the hydraulic gradient in homogeneous soil in the case with no macropores is 0.74. The value of K that would need to be multiplied with this quantity to give a discharge velocity of 26 mm/hr is 35 mm/hr. From this we conclude that the hydraulic conductivity of the sand used in the experiments was 35 mm/hr.

Considering experiment B, we find that in the absence of macropores a discharge velocity of 11 mm/hr was realized. From the FD simulations, the hydraulic gradient in the clay layer of the non-homogeneous soil, in the absence of macropores, is 0.77. The value of K which would then give a discharge velocity of 11 mm/hr is 14 mm/hr. Hence we conclude that the saturated hydraulic conductivity of the less permeable layer was 14 mm/hr. Noting that the ratio of experiment A final infiltration capacity to experiment B final infiltration capacity is 26:11, assuming that the saturated hydraulic conductivities will be in the same ratio, we could calculate the K of the less permeable material knowing that of the more pervious material.

$$35 : K(l) = 26 : 11$$

Therefore K(l), or the hydraulic conductivity of the less pervious medium equals 14 mm/hr. This is the same value obtained by using information from the finite difference simulation for a two-layer soil profile. Generally speaking, increasing number of macropores tends to increase the rate of soil

Table 6.4: Change of Basic infiltration capacity with N, Data B

N	0	4	8	12	14	16	18	20	22	24
f_c	11	14	17	20	23	22	23	23	26.6	26.7

Table 6.5: Discharge Velocities (Homogeneous Soil) mm/hr

N	Case 1	Case 2
0	35.0	26.0
4	37.0	26.7
8	39.0	28.0
12	41.0	29.0
16	42.0	29.5
20	43.0	30.1
24	45.0	30.23

water uptake. This would consequently also increase the discharge velocities. The hydraulic gradients only depend on the boundary conditions. In other words the flow net of the section depends on the boundary conditions and not on the saturated hydraulic conductivity. The latter would only influence the discharge velocities. Table 6.5 and 6.6 show the discharge velocities that would be realized considering that the more permeable material has a hydraulic conductivity $K_2 = 35$ mm/hr and the less permeable has $K_1 = 14$ mm/hr.

Table 6.6: Discharge Velocities (Non-homogeneous Soil) (mm/hr)

N	Case 3	Case 4
0	14.0	10.8
2	14.8	11.9
4	15.5	12.7
6	16.4	13.2
8	16.8	13.4
10	17.2	13.6

6.3 Change of Saturated Hydraulic Conductivity With Macropores

Table 6.7 shows the comparison of the observed experimental equilibrium infiltration capacity against FD simulations of discharge velocity in homogeneous material. The calculation of saturated hydraulic conductivity in the absence of macropores has been explained in section 6.2. Comparing the FD simulations for homogeneous soil we realize that other than for N=0, the values of V and f_c are not the same. The reason could be that, the dimensions of macropores used in the experiments was not the same as the ones used in the FD simulations.

By regression analysis, it was found that V and experimental f_c are linearly related, with a slope of 7.2.

$$f_c = 7.2V - 162.5 \tag{6.2}$$

If we assume that V is also linearly related to saturated hydraulic conductivity and that the slope of the linear relationship is also 7.2, since the value

Table 6.7: Determining Hydraulic Conductivity of Homogeneous Soil (Exp.A)

N	V (mm/hr)	Expt. Basic infil. cap.(mm/hr)	Hyd. conduc. K (mm/hr)
0	26	26	35
4	26.7	31	40
8	28	35	49.4
12	29	48	56.6
16	29.5	53	60.2
20	30.1	54	64.5
24	30.2	55	65.2

of K at N=0 is known, then K can be calculated for other levels of macroporosity. Table 6.7 and Figure 6.5 show the variation of K with N. This is true only if the change in macroporosity actually changed the hydraulic conductivity of the soil.

6.4 Performance of Infiltration Equations

The performance of Horton, Kostiakov, and Philip equations were compared using the coefficient of determination R^2, and a fitting efficiency criterion.

Tables 6.8 and 6.9 show the various values of the coefficient of determination obtained for the different equations. Data A was found to give very low values of R^2, relative to the R^2 given by data B. For data A, Hor-

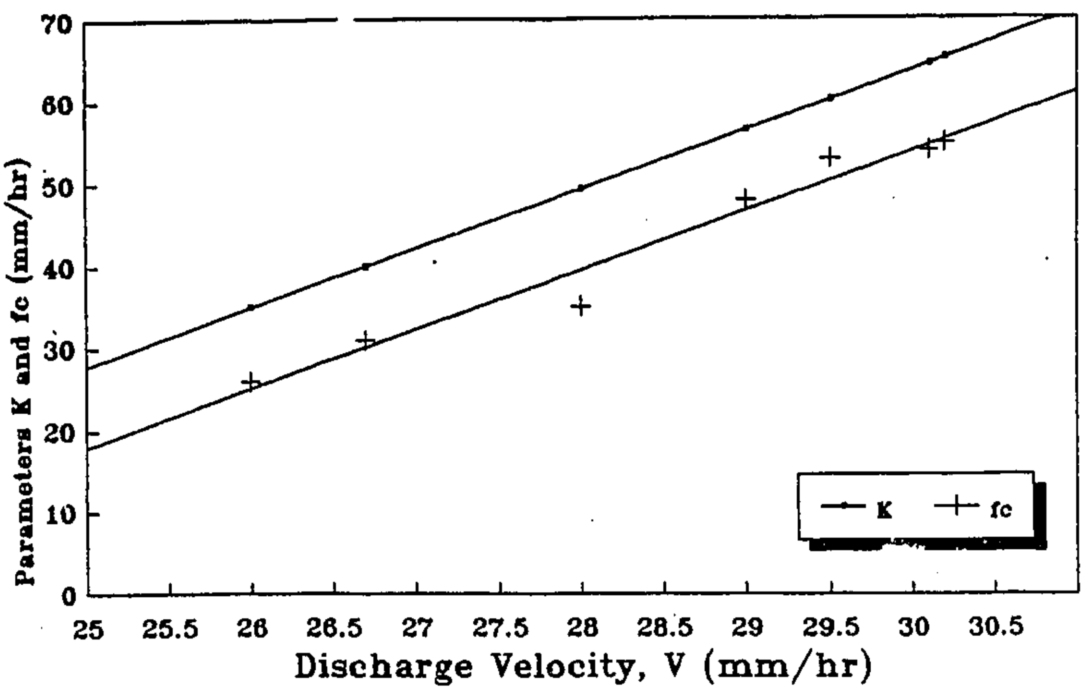

Figure 6.5: Variation of (K) and f_c with V

ton equation gave the lowest values of R^2. All equations gave comparable values of R^2 for data B.

In terms of fitting efficiency, (E) as shown in Tables 6.10 and 6.11, Data B fitted the equations with higher efficiencies. This efficiency also varied from equation to equation but with respect to fitting infiltration capacity, Horton equation seems to have the smallest values of E. From fitting efficiency viewpoint, Philip equation has the best performance since it gives the highest efficiency more times than any of the other equations. The capability of the equations to predict total infiltrated volume was also investigated.

Table 6.8: Data A-Regression Coefficient R^2

N	Horton	Philip	Kostiakov
0	0.03	0.59	0.43
4	0.09	0.49	0.36
8	0.12	0.53	0.40
12	0.38	0.77	0.75
16	0.86	0.65	0.78
20	0.49	0.22	0.26
24	0.12	0.68	0.63

Table 6.9: Data B-Regression Coefficient R^2

N	n	Horton	Philip	Kostiakov
0	0.00	0.87	0.87	0.87
2	0.08	0.83	0.79	0.78
8	0.33	0.73	0.84	0.81
12	0.50	0.77	0.81	0.78
14	0.58	0.89	0.74	0.77
16	0.67	0.81	0.86	0.84
18	0.75	0.97	0.86	0.86
20	0.83	0.88	0.88	0.86
22	0.92	0.95	0.83	0.81
24	1.00	0.90	0.85	0.83

Table 6.10: Data A-Fitting Efficiency E %

N	Horton	Philip	Kostiakov
0	-1.00	59.0	47.5
4	4.80	48.6	37.5
8	12.6	52.0	42.4
12	62.6	76.5	76.6
16	78.9	65.3	77.5
20	20.2	21.8	23.3
24	29.3	68.1	64.2

Table 6.11: Data B-Fitting Efficiency E %

N	n	Horton	Philip	Kostiakov
0	0.00	68.6	85.6	86.9
2	0.08	62.1	78.5	78.6
8	0.33	62.5	87.8	84.7
12	0.50	60.5	85.7	80.0
14	0.58	62.6	74.2	71.0
16	0.67	75.2	86.3	83.6
18	0.75	81.8	85.8	83.6
20	0.83	78.3	87.6	85.7
22	0.92	81.3	82.6	78.5
24	1.00	90.1	85.3	81.7

6.4.1 Prediction of Cumulative Infiltration

Observed cumulative infiltration was computed by the summation method as explained in chapter 5. Computation of simulated cumulative infiltration is done by plugging in the appropriate equation parameters into the cumulative form of the equation. When the usual forms of the equations were used, only Horton equation produced reasonable results. Large errors in predicting total infiltration were made by the other equations. This is clearly seen in Tables 6.12 to 6.14. Figures 6.6 and 6.7 illustrate that Philip and Kostiakov equations simulate infiltration curves that are parallel to the curve of observed cumulative infiltration. They tend to overestimate total infiltration by a certain constant. This suggests that a shift of the simulated cumulative infiltration curve downwards would bring it closer to the observed cumulative infiltration curve. Then, the error made in predicting cumulative infiltration would be smaller. This calls for a modification of Philip and Kostiakov equations. A modification was effected by adding a constant to the cumulative form of each of the equations. The following are the suggested new forms.
Philip equation, for t being greater than 0 :

$$F = St^{1/2} + At + D \tag{6.3}$$

Kostiakov equation, for t being greater than 0 :

$$F = \frac{A}{B+1}t^{B+1} + C' \tag{6.4}$$

At t=0, total infiltration F = 0, for both Kostiakov and Philip equations. After calibration, the constants were determined. A summary is given in Tables 6.15 and 6.16.

Table 6.12: Horton Equation Parameters and Error in Predicted Total Infiltration Fs for Data B

N	n	k	f_c (mm/hr)	Fo (mm/hr)	F (mm)	Fs (mm)	Error
0	0.00	4.29	11	61.6	23.1	22.6	2%
2	0.08	4.29	14	62.1	26.0	25.1	4%
8	0.33	4.97	17	62.4	27.3	26.1	5%
12	0.50	4.50	20	54.2	28.5	27.5	3%
14	0.58	3.83	23	59.2	34.0	32.2	5%
16	0.67	3.48	22	48.4	29.3	29.4	0%
18	0.75	5.03	23	71.2	32.5	32.5	0%
20	0.83	5.67	23	71.1	31.8	31.5	1%
22	0.92	5.58	26.6	72.8	35.0	34.8	0%
24	1.00	5.77	26.7	79.0	34.4	35.7	-4%

Table 6.13: Philip Equation Parameters and Error in Predicted Total Infiltration Fs, for Data B

N	n	0.5S	C (mm/hr)	F (mm/hr)	Fs (mm)	Error (mm)
0	0.00	27.4	-24.7	23.1	30.1	-30%
2	0.08	29.3	-24.4	26.0	34.2	-32%
8	0.33	25.6	-15.3	27.3	35.9	-32%
12	0.50	20.3	-5.50	28.5	35.1	-23%
14	0.58	20.6	-1.70	34.0	39.5	-16%
16	0.67	15.0	5.40	29.3	35.4	-21%
18	0.75	19.8	0.30	32.5	39.9	-23%
20	0.83	19.7	0.10	31.8	39.5	-24%
22	0.92	17.3	6.30	35.0	40.9	-17%
24	1.00	15.9	8.50	34.4	40.3	-17%

From table 6.16 the absolute value of constant C' that needs to be added gets smaller as the number of macropores increases. The more pervious the soil is, the less the value of constant C'. In fact, examining data A, it is found that no constant needs to be added to Kostiakov equation.

The average value of modified Philip constant D is smaller for data A, than it is for data B. Tables 6.16 to 6.19 show the analysis of error made in predicting total infiltration for data A.

Data B was used to investigate the effect of macroporosity on equation parameters. Equation parameters changed with changing M-index. The following equations express equation parameters as functions of M-index

Table 6.14: Kostiakov Equation Parameters and Error in Predicted Total Infiltration Fs, for Data B

N	n	A	B	F (mm)	Fs (mm)	Error
0	0.00	9.12	-0.82	23.1	50.7	-119%
2	0.08	11.4	-0.76	26.0	47.4	-82%
8	0.33	13.6	-0.66	27.3	40.0	-47%
12	0.50	17.0	-0.50	28.5	34.0	-19%
14	0.58	21.0	-0.44	34.0	37.5	-10%
16	0.67	21.1	-0.36	29.3	33.0	-13%
18	0.75	21.1	-0.44	32.5	37.7	-16%
20	0.83	20.7	-0.44	31.8	37.0	-16%
22	0.92	24.4	-0.35	35.0	37.5	-7%
24	1.00	24.9	-0.33	34.4	37.2	-8%

Table 6.15: Performance of Modified Philip Equation-Data B

N	n	0.5S	C	D	F (mm)	Fs (mm)	Error
0	0.00	27.4	-24.7	-8.8	23.1	21.3	8.0%
2	0.08	29.3	-24.	-10	26.0	24.2	7.0%
8	0.33	25.6	-15.3	-9.0	27.3	26.9	1.0%
12	0.50	20.3	-5.50	-7.0	28.5	28.1	1.0%
14	0.58	20.6	-1.70	-6.5	34.0	33.0	3.0%
16	0.67	15.0	5.40	-6.0	29.3	29.4	0.0%
18	0.75	19.8	0.30	-7.0	32.5	32.9	-1.0%
20	0.83	19.7	0.10	-7.5	31.8	32.0	-1.0%
22	0.92	17.3	6.30	-9.0	35.0	31.9	9.0 %
24	1.00	15.9	8.50	-10	34.4	30.3	12.0%

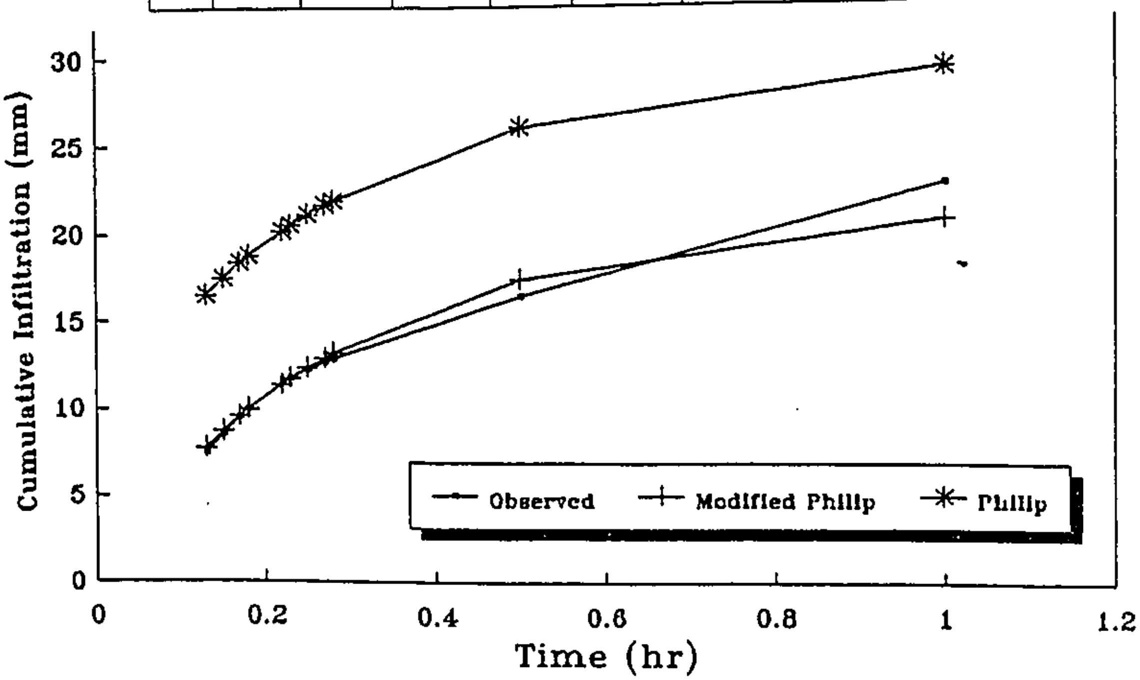

Figure 6.6: Performance of Modified Philip Equation-Data B

Table 6.16: Performance of Modified Kostiakov Equation-Data B

N	n	A	B	C'	F (mm)	Fs (mm)	Error
0	0.00	9.12	-0.82	-27.5	23.1	23.2	-0 %
2	0.08	11.4	-0.76	-21.0	26.0	26.4	-1.0%
8	0.33	13.6	-0.66	-13.0	27.3	27.0	1.0%
12	0.50	17.0	-0.50	-5.0	28.5	29.0	-2.0%
14	0.58	21.0	-0.44	-3.5	34.0	34.0	-0 %
16	0.67	21.1	-0.36	-3.0	29.3	30.0	-2.0%
18	0.75	21.1	-0.44	-4.5	32.5	33.2	-2.0%
20	0.83	20.7	-0.44	-5.0	31.8	32.0	-1.0%
22	0.92	24.4	-0.35	-2.5	35.0	35.0	0 %
24	1.00	24.9	-0.33	-2.5	34.4	34.7	-1.0%

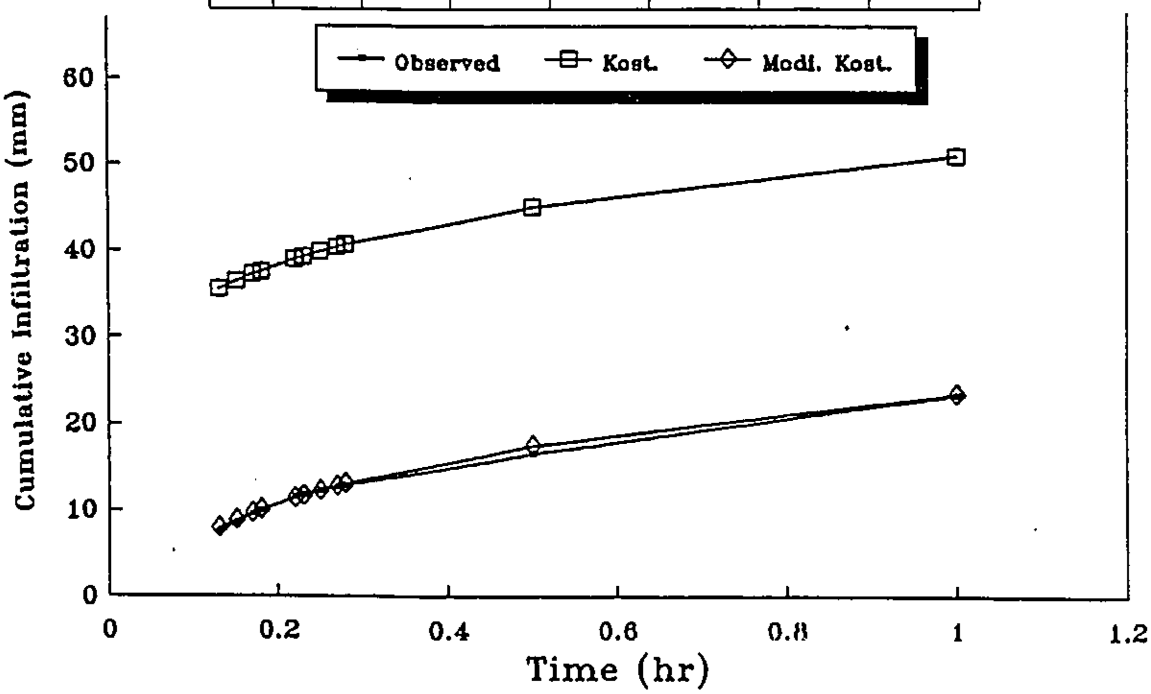

Figure 6.7: Performance of Modified Kostiakov Equation-Data B

Table 6.17: Horton Equation Parameters and Error in Predicted Total Infiltration Fs, for Data A

N	k	f_c (mm/hr)	Fo (mm/hr)	F (mm)	Fs (mm)	Error
0	0.58	26	31.3	32.2	30.0	7%
4	0.78	31	35.9	36.6	34.4	6%
8	0.40	35	39.9	40.0	39.0	2%
12	1.64	48	57.6	53.3	52.7	1%
16	2.37	53	63.9	56.9	57.2	0%
20	1.98	54	61.4	57.6	57.2	1%
24	0.95	55	57.2	56.9	56.4	1%

Table 6.18: Performance of Modified Philip Equation-Data A

N	0.5S	C	D	F (mm)	Fs (mm)	Error
0	7.1	19.8	-2.0	32.2	32.0	1.0%
4	6.4	24.6	-1.5	36.6	36.9	2.0%
8	5.0	31.2	-1.5	40.0	39.7	1.0%
12	4.7	45.5	-1.5	53.3	53.4	0.0%
16	2.8	52.3	-1.0	56.9	56.9	0.0%
20	4.0	51.5	-2.0	57.6	55.6	-7.0%
24	1.5	54.3	-0.5	56.9	56.4	-2.0%

Table 6.19: Performance of Modified Kostiakov Equation-Data A

N	A	B	C'	F (mm)	Fs (mm)	Error
0	27.3	-0.15	0	32.2	32.1	0 %
4	31.4	-0.12	0	36.6	35.7	3.0%
8	36.4	-0.08	0	40.0	39.6	1.0%
12	49.6	-0.08	0	53.3	53.9	-1.0%
16	54.5	-0.05	0	56.9	57.4	-1.0%
20	55.2	-0.05	0	57.6	58.1	-1.0%
24	55.7	-0.02	0	56.9	56.8	0.0%

for the conditions found in this laboratory investigation.

Horton equation parameters

$$f_c = 14.3n + 12.8 \tag{6.5}$$

$$f_0 = 13.9n + 56.3 \tag{6.6}$$

$$k = 1.3n + 4.0 \tag{6.7}$$

Philip equation parameters

$$A = 35n - 25 \tag{6.8}$$

$$0.5S = -12.8n + 28 \tag{6.9}$$

Kostiakov equation parameters

$$A = 16n + 10 \tag{6.10}$$

$$B = 0.5n - 0.8 \tag{6.11}$$

Calculating each infiltration parameter for changing macropore populations is undesirable. Instead it is better to have a term in the infiltration equations to represent the influence of the macroporous conditions. Presented below is a new form of Horton equation capable of calculating total infiltration when the current M-index and the basic infiltration capacity for the non-macroporous condition are known.

6.5 Modified Horton Equation

The proposed model accounts for flow through both the matrix and macropore domains. Matrix domain flow can be described by using any of the classic infiltration equations, such as Richard's, Horton, Philip and Kostiakov equations. In this document, the Horton equation is selected since it is the most used empirical infiltration equation. A general form of the suggested equation is

$$F = F_{mi} + F_{ma} \tag{6.12}$$

F is the total infiltrated volume at a given time. F_{mi} and F_{ma} are the total infiltration through the matrix and macropore domains respectively.

While it is relatively easy to model infiltration through the non-macroporous soil, it becomes more difficult to model this process in the presence of macropores. Equation parameters change with changing M-index. This makes it necessary to calibrate the equation every time there is a change in macroporosity. However, it would be preferable if an equation such as Horton

Table 6.20: Variation of F1 with M-index

M-index	F1 (mm)	F_{ma} (mm)	E (%)
0	23.3	0	92.6
0.1	26.0	2.7	90.3
0.3	27.3	4.0	96.3
0.5	28.5	4.8	99.8
0.6	34.0	10.7	92.0
0.67	29.3	6.0	95.6
0.75	32.6	9.3	99.1
0.83	31.8	8.5	99.9
0.92	35.0	11.7	99.0
1.00	34.4	11.1	99.4

equation could be calibrated once for a given watershed . Then further variation in macroporosity with time could be accounted for.

Assuming that the total infiltration through the soil matrix can be modelled by the usual Horton equation (i.e equation 2.2), it follows that

$$F_{mi} = f_c\,t - \frac{(fo - f_c)}{k}(e^{-kt} - 1) \qquad (6.13)$$

F_{ma}, which represents total infiltration through the macropore domain, is referred to as "bypass" and is treated as a parameter of equation 6.18. Table 6.20 shows total infiltration (F1) at time t=1 hr, for various values of M-index (n). If the F for M-index of 0 is taken as the infiltration through the soil matrix (F_{mi}), bypass can be calculated as

$$F_{ma} = F - F_{mi} \qquad (6.14)$$

From Figure 6.8, bypass increases linearly with macropore index. Figure 6.9 shows the variation of bypass with respect to both time and M-index.

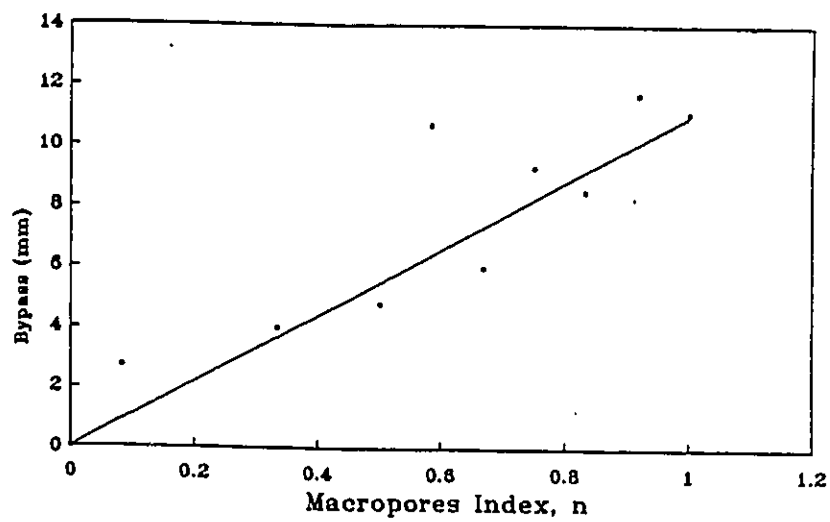

Figure 6.8: Variation of Bypass with M-index

As time increases, the total volume of bypass increases. The relationship between F_{ma} $and\, n$ was found to be

$$F_{ma} = 11n \tag{6.15}$$

From equations 6.18 and 6.19

$$F = f_c\, t - \frac{(f_o - f_c)}{k}(e^{-kt} - 1) + (11n)t \tag{6.16}$$

A more general form of the equation above would be

$$F = f_c\, t - \frac{(f_o - f_c)}{k}(e^{-kt} - 1) + (\alpha\, n)t \tag{6.17}$$

The infiltration capacity form of modified Horton equation would be

$$f = f_c + (f_o - f_c)e^{-kt} + (\alpha\, n) \tag{6.18}$$

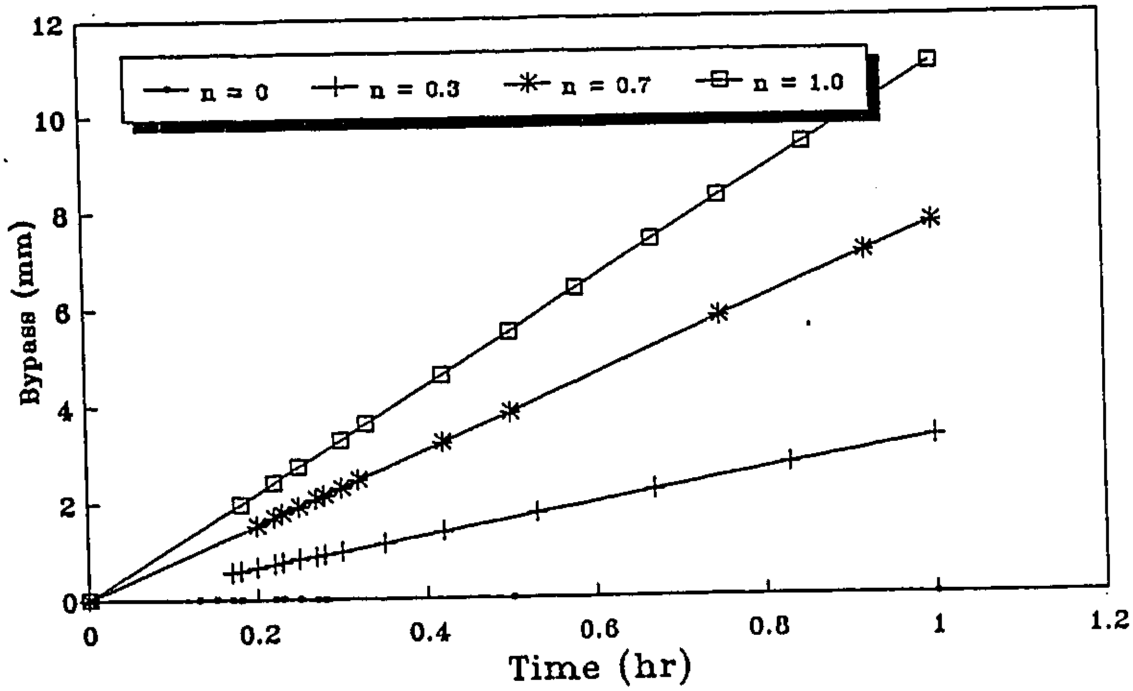

Figure 6.9: Variation of Bypass with Time and M-index

The symbol α is a parameter that would be expected to vary from watershed to watershed. For a particular watershed, α can only be obtained through calibration. This would involve fitting the equation to observed infiltration for known macropore indices. To test the goodness of the new infiltration model, equation 6.22 was applied to the observed data for different values of n. The values of Horton equation parameters f_c, f_o, $and\, k$ for the no macropore case were used in all cases. These parameters were determined by fitting the infiltration capacity form of the equation to the observed infiltration capacity data. The values of the parameters in the absence of macropores were found to be 11 mm/hr, 61.6 mm/hr and 4.29, respectively. From the appearance of Figure 6.10 and the high fitting efficiencies shown in Table 6.20, it is clear that the equation fits the observed data fairly well. It was unnecessary to determine parameters at different levels of macroporosity, as long the parameters in the no macropore case were known.

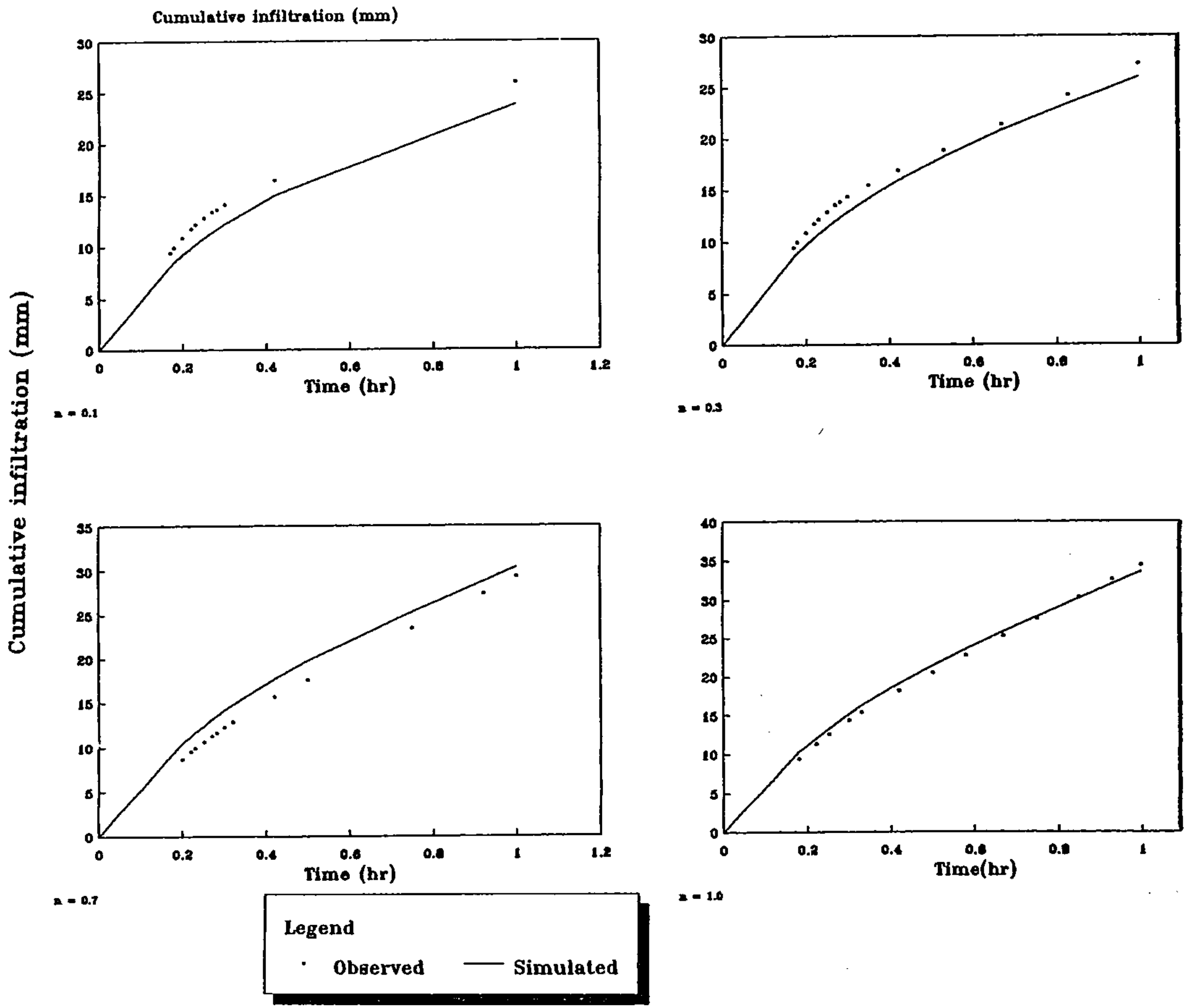

Figure 6.10: Fitting Equation on Cumulative Infiltration for Various Values of M-index

6.6 Runoff and Tile Flow

From experiments A and B, the presence of macropores has been found to affect the following.

1. The volumes of tile flow and runoff realized from the one hour rainfall.
2. The time to peak for both runoff and tile flow hydrographs.
3. Volume of infiltrated water that goes into deep percolation.
4. Tile and runoff flow peaks

These observations are further discussed in below.

6.6.1 Effect of Macropores on Runoff and Tile Flow

The total infiltrated volume produced in a one hour rainfall, was found to increase with increasing macropore index. Since in all cases rainfall was applied at about the same level of soil moisture,the volume of tile flow also increased as macroporosity increased. The total runoff volume decreased with macroporosity (see Figure 6.11). Hence it appears that the presence of macropores increases soil water acceptance capacity. This could be because the water finds an easier path into the tile drain and that there is a larger surface area for infiltratión, so within the one hour more water can infiltrate. These reasons explain why the above volumes increase with increasing macropore index. The path to the final destination is made shorter. For this reason we expect more water to find its way into the soil.

Runoff peaks are reached earlier than tile flow peaks. As the number of macropores increases, runoff time to peak increases. Lack of precision in measurements seems to cause irregularities, which make the trend of changes difficult to judge. Looking at the scatter of time to peak against macropore index (for data B), it is found that generally speaking, runoff

Table 6.21: Total Runoff, Tile flow, Infiltration and Percolation for Data B

N	n	Tile	Runoff	Infiltration	Perc.(P%)
0	0.00	7.7	47.1	12.9	60.0
2	0.08	7.3	40.5	19.5	37.0
8	0.33	10.4	37.2	22.8	46.0
12	0.50	12.3	33.5	26.5	46.0
14	0.58	15.6	30.0	30.0	52.0
16	0.67	15.4	30.4	29.6	52.0
18	0.75	14.1	30.2	29.8	47.0
20	0.83	15.4	31.1	28.9	53.0
22	0.92	18.1	27.6	32.4	56.0
24	1.00	19.0	27.7	32.3	59.0

time to peak is less than tile flow time to peak. From the two sets of data, it is clear that tile flow time to peak does not vary a lot. It remains at around 1 hr. This coincides with the rainfall period. Runoff time to peak seems to increase as the number of non-capillary pores is increased. Peak tile flow decreases with macropore index. The change is clearly seen in Figure 6.11, derived from data B. Peak runoff increases with increasing macropore index. From these results it can be said that as number of macropores increases the subsurface drainage system receives larger volumes of water. From table 6.21 it can be seen that increasing macroporosity increases the percentage of rainfall that percolates. This is because there is an increase in the bypass of the soil matrix. In this work, percolation was taken to be as the fraction of infiltrated water which reaches the tile drain. P(%) linearly increases with macropore index.

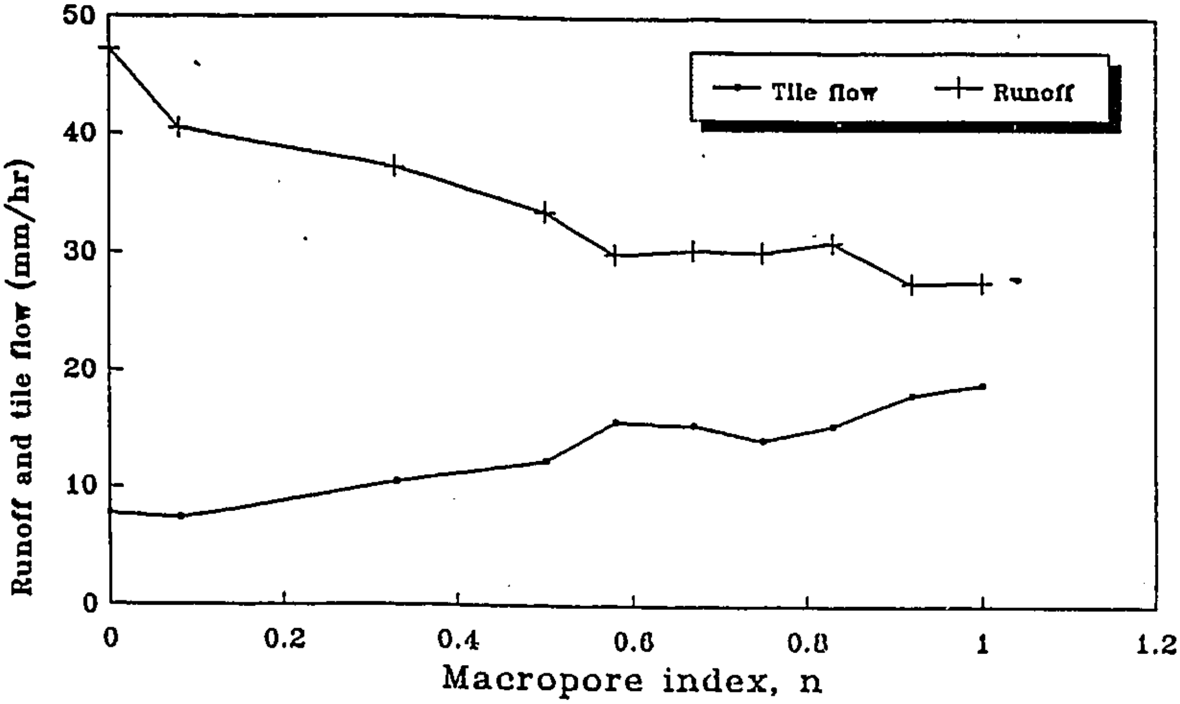

Figure 6.11: Change of Total Tile Flow and Runoff Volumes With Macropore Index (Data B)

Table 6.22: Variation of Peak Flow and Time to Peak-Data A

N	Runoff Peak	Runoff time to peak	Tile flow Peak	Tile flow time to Peak
0	24	0.33	17.4	0.82
4	27.6	0.25	33.6	1.00
8	23.4	0.25	29.4	1.03
12	10.5	0.50	16.5	0.97
16	4.85	0.72	22.5	1.17
20	5.76	0.30	46.5	0.98
24	9.60	0.30	28.5	0.58

Table 6.23: Variation of Peak Flow and Time to Peak-Data B

N	n	Tile Peak	Tile time to peak(hr)	Runoff Peak	Runoff time to Peak(hr)
0	.00	9.0	1.2	48.0	1.0
2	.08	10.0	1.0	45.0	0.4
8	.33	13.5	1.0	42.0	0.4
12	.50	15.3	1.0	39.0	0.5
14	.58	19.2	1.0	30.0	1.0
16	.67	18.0	1.0	36.0	0.5
18	.75	16.5	1.0	36.6	0.9
20	.83	19.2	1.0	36.9	1.0
22	.92	21.0	1.0	33.3	1.0
24	1.00	21.3	0.9	34.2	0.9

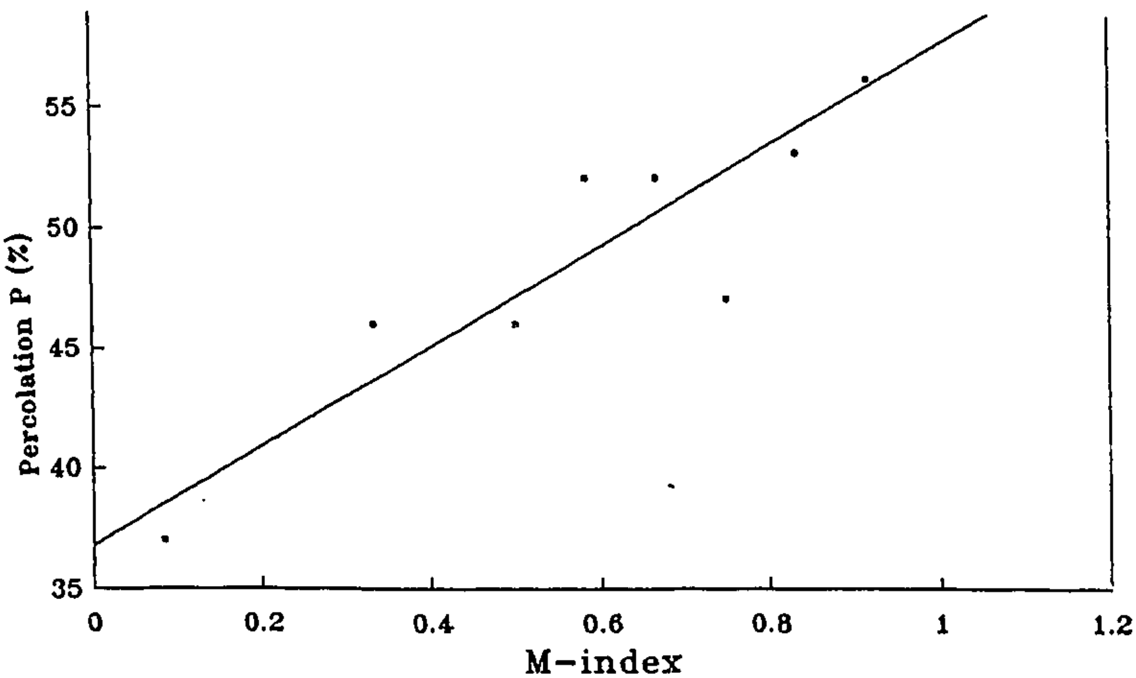

Figure 6.12: Influence of Macropores on Percolation

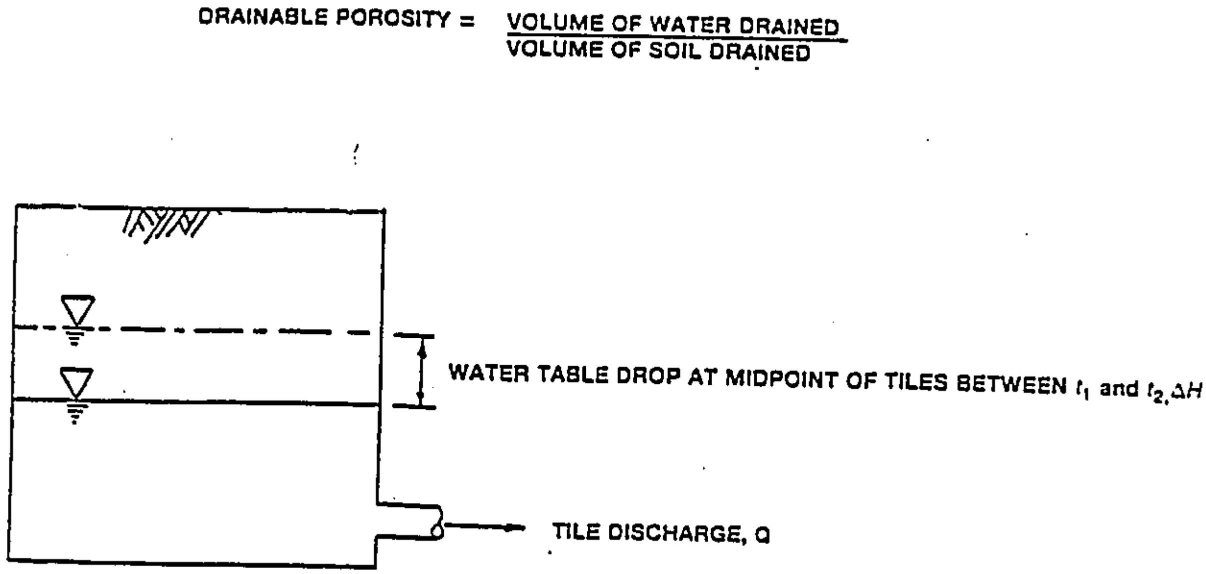

Figure 6.13: Determination of Drainable Porosity

6.6.2 Drainable Porosity

One of the important parameters in the model TILE is drainable porosity (P_d%). Defined as the maximum water available through gravity drainage, it is the ratio of water lost from the soil to the volume of soil drained. This represents the difference between the saturated moisture content and the field capacity. It was calculated as the ratio of total depth of water drained from the soil during the time from beginning of flow until peak tile flow is reached to the total depth of the soil profile (50cm). It was assumed that the water table lowered from the soil surface to the bottom of the tank within the two hours tile flow was monitored. P_d was found to increase as macropore index increased. This is reasonable since an increase in macropores should provide more space where gravity water can be stored. Table 6.24 and Figure 6.14 show how drainable porosity changes with macropore index.

Table 6.24: Variation of Drainable Porosity with Macropore Index "n"

N	n	Drainable porosity %
0	.00	1.1
2	.08	1.1
8	.33	1.4
12	.50	1.5
14	.58	1.7
16	.67	2.0
18	.75	2.0
20	.83	2.0
22	.92	2.2
24	1.00	2.3

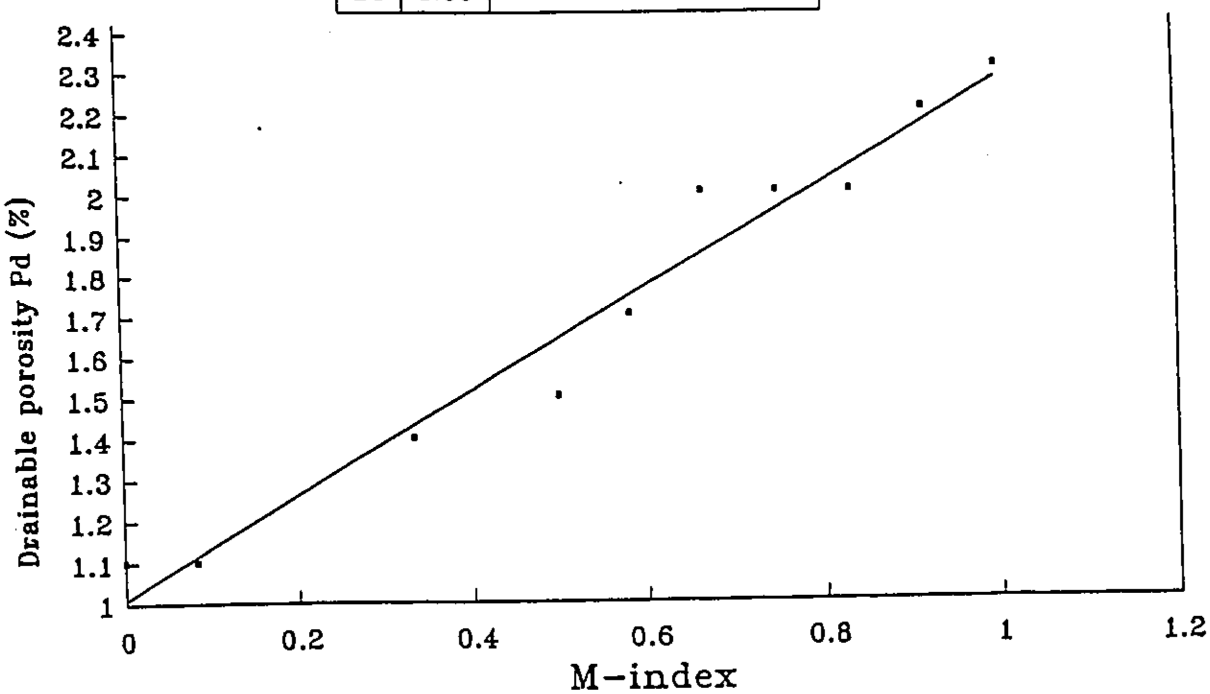

Figure 6.14: Variation of Drainable Porosity with Macropore Index "n"

6.6.3 Comparison of Observed Runoff and Tile Flow with TILE Model Simulations

It has been shown that the presence of macropores affects the quantity of surface runoff and tile flow produced after a rainfall event. Many hydrologic models such as TILE do not take macropores into account. The computer program TILE was used to simulate some runoff and tile flow data. The difference between simulated data and observed data was evaluated for varying M-index for experiment B data. The field for the model was assumed to be ten times the size of the laboratory soil bed. This made it possible to have numbers that more likely would be used in the field. For example instead of inputting 1 row of laterals, an input of 10 was made. The data in table 6.27 was input: TILE has no means of accounting for change in soil macroporosity. The effect of using the macropore-free soil parameters is shown in Table 6.26 and Figures 6.15 to 6.17.

The only way to make TILE reflect varying M-index in the soil is to change its parameters accordingly. Some parameters are constants and do not vary with increasing volume of macropores. A quantity like saturated hydraulic conductivity is not supposed to vary since it is a function of the soil matrix. However, in reality, increasing macropores seems to change the apparent saturated hydraulic conductivity. In this case it was assumed that there was no way to tell what the new values of parameters were. In general, it is too expensive and time-consuming to determine the time variation of the model parameters.

Table 6.25: TILE Model Parameters

Parameter	Value
Diameter of drains(mm)	100
Effective radius	0.005
Spacing of drains (m)	1
Number of laterals	10
Length of drains (m)	20
Surface slope	0.005
Surface flow length (m)	20
Coefficient of permeability (m/day)	0.34
Depth of impermeable layer from drain axis (m)	0.050
Drainable porosity (%)	1.1 (value at M-index = 0)
Max. depression storage (mm)	1
Initial moisture content (%) (for both upper and lower layers)	26
Field capacity (%) (for both upper and lower layers)	27
Final infiltration capacity f_c (for both upper and lower layers (mm/hr))	11 (Value at M-index = 0)
Depth-upper layer (mm)	500
Depth-lower layer (mm)	0.0

Table 6.26: Comparison of Observed and TILE Simulated Quantities

	Runoff Volume (mm)		*Total Peak Flow (mm/hr)*		*Tile Volume (mm)*	
N	Observed	Simulated	Observed	Simulated	Observed	Simulated
0	47.08	48.5	57.0	46.4	7.23	6.50
8	37.24	48.5	55.5	46.4	10.38	6.50
12	33.47	48.5	54.3	46.4	12.29	6.50
16	30.37	48.5	54.6	46.4	15.39	6.50
22	27.67	48.5	54.3	46.4	18.06	6.50
24	27.7	48.5	55.5	46.4	19.00	6.50

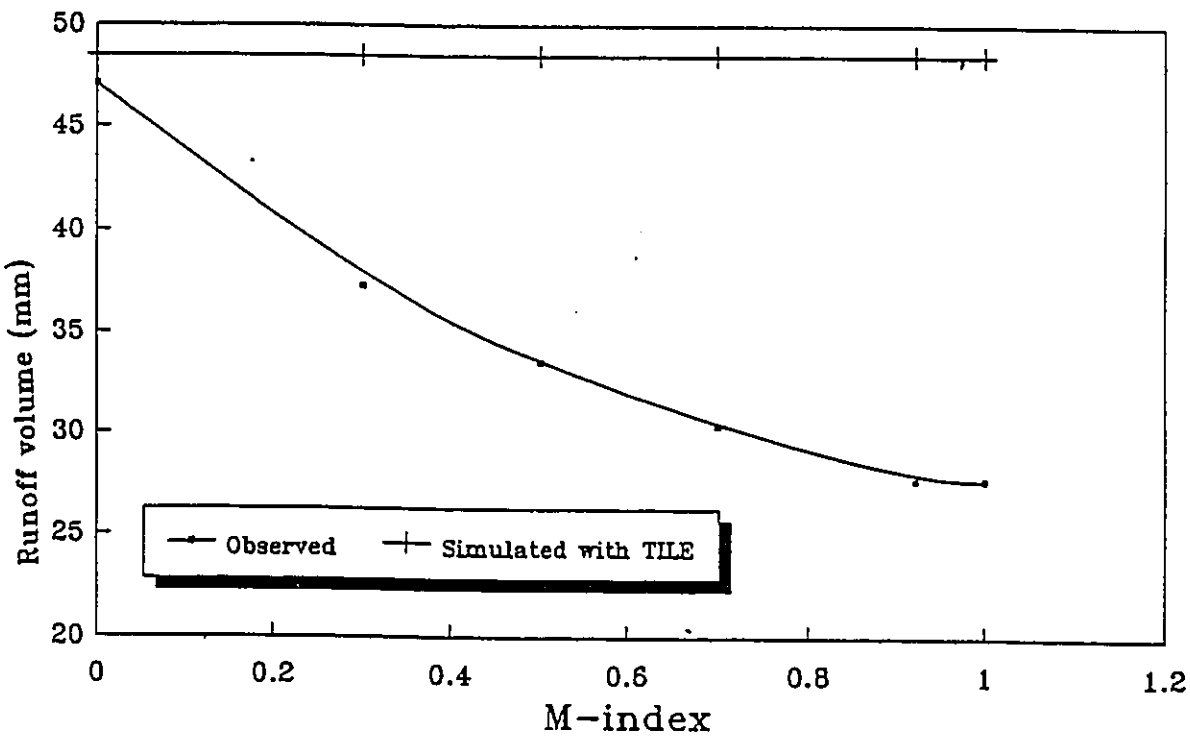

Figure 6.15: TILE Performance in Runoff Volume Simulation

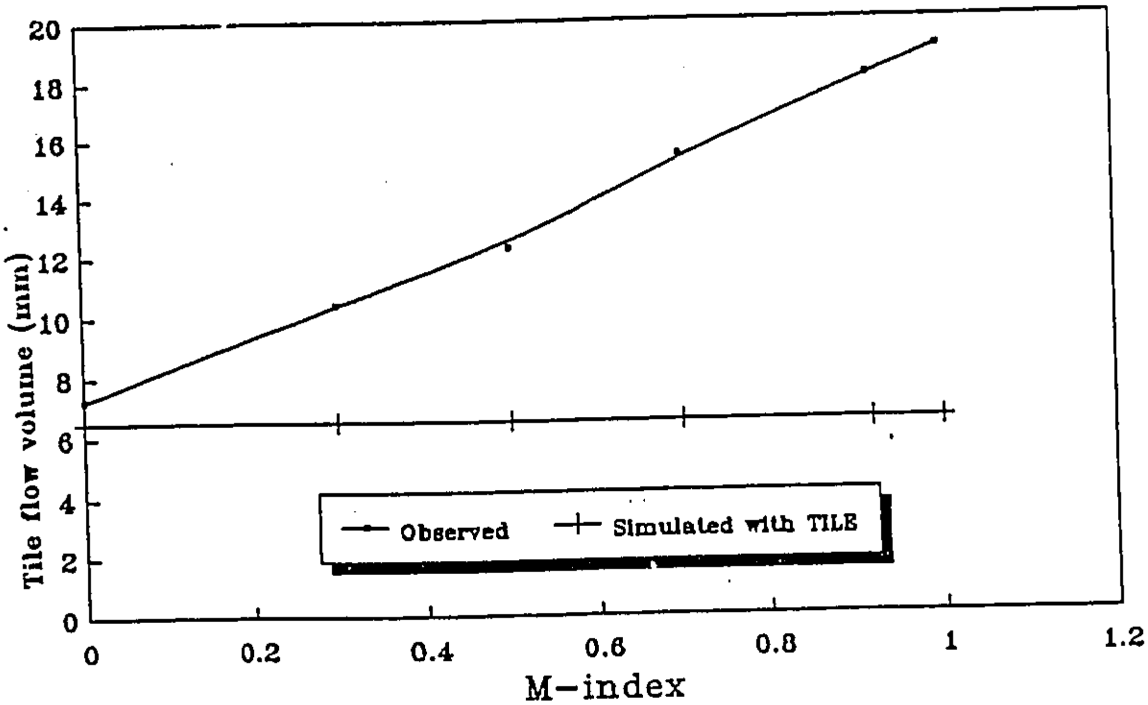

Figure 6.16: TILE Performance in Tile Flow Volume Simulation

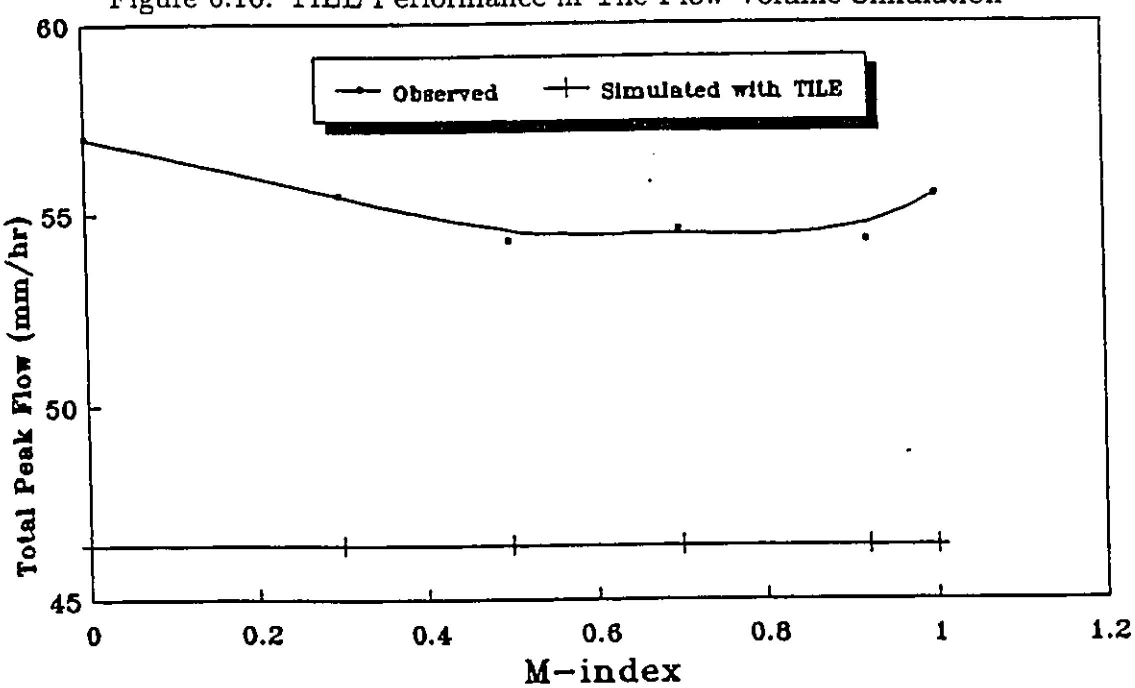

Figure 6.17: TILE Performance in Total Peak Flow Simulation

As can be seen in Table 6.26 and Figures 6.15 to 6.17:

1. The accuracy of TILE to predict runoff volume, tile volume and total peak flow decreases with M-index. The error made, when using parameters in the non-macroporous condition, increases with M-index. This is because even though model parameters vary with time, no adjustments are made on the calculations.

2. TILE tends to overestimated runoff volume.

3. The model underestimates tile flow and total peak flow which is comprised of runoff and tile flow.

TILE is meant to simulate hydrologic response of agricultural drainage on a basin scale, and to lead to a properly designed system. A hydrograph for a drained area will exhibit higher peak flows and a faster recession than the undrained case (Paine and Watt, 1988). Higher velocities and discharges could lead to increased erosion and frequency of flooding in drainage channels and receiving water ways. For this reason underestimation of total peak flow, as is the case above, may lead to overloading of the surface drainage network and probably lead to unnecessary floods and erosion of waterways.

TILE inaccuracy may be attributed to the fact that Holtan equation does not simulate infiltration accurately enough with changing macroporosity. Therefore an equation that takes into account changes in macroporosity, as was developed in this thesis, should be used.

Chapter 7

CONCLUSIONS AND RECOMMENDATIONS

Conclusions

1. From the finite difference simulations, it can be said that when an impermeable horizontal barrier is close to the soil surface, basic infiltration capacity (f_c) is not an accurate estimate of saturated hydraulic conductivity (K) of the soil.

2. Equation parameters have been found to change with changing macroporosity. For example basic infiltration rate tends to increase with increasing number of macropores. This observation has been used to develop the concept of macropore index called M-index. It quantifies soil macropores more conveniently than using numbers of macropores.

3. Philip and Kostiakov infiltration equations have been found to fit instantaneous infiltration with higher values of R^2 and E than Horton

equation, which has been shown by Singh and Buapeng (1977) to be a better infiltration equation. However, Horton equation gives a better performance in the fitting of cumulative infiltration. Modified forms of Philip and Kostiakov cumulative infiltration equations have a better performance than the unmodified forms. It is concluded that Philip and Kostiakov equations when modified would give more satisfactory simulations of infiltration than Horton equation since the modification improves the quality of simulated cumulative infiltration without affecting the ability of the equations to simulate instantaneous infiltration. This, however, needs to be tested with field data.

4. Taking into consideration the M-index, a modified form of Horton equation has been developed. This is an equation that requires the infiltration parameters before the development of macropores and the current M-index.

5. An increase in the M-index increases percolation which is reflected by the increased volume of tile flow. As a result of increased soil water uptake, when the M-index increases, the volume of runoff generated decreases. Thus hydrologic models ignoring macroporosity can be expected to be less accurate than those which do.

Recommendations

- It is recommended that the minimum depth of impermeable barrier required for f_c to be considered as an accurate estimate of K be determined in a further study.

- In watersheds where infiltration patterns are likely to vary with time, values of M-index should be determined for different time periods.

This will quantify macropore populations for the different times and make it possible to model infiltration and other hydrologic processes.

- The modified equations should be tested with field data in a basin with detailed knowledge of the macropores in order to transfer the findings of the study to the practical world.

- It has been shown that the increases in volumes of water reaching tile drains is associated with bypass flow, which is significantly influenced by macroporosity. Since increased bypass flow might have an effect on the transport of dissolved solutes, further research is required to determine the usefulness of the M-index concept in the modelling of solute transport and prediction of quantity of leached pollutants that are able to reach the ground water reservoir.

- Some of the parameters used in the tile drainage model TILE, such as f_c and drainable porosity, have been noticed to increase significantly with increasing M-index. Unless changes in the physical characteristics of the soil are well noted, and model parameters adjusted accordingly, large errors could be made when TILE is used to simulate runoff and tile flow volumes in the presence of macropores. Holtan equation used in the model should have the capability to account for the presence of macropores. The equation should be therefore modified in a manner similar to the Horton equation in this work, so that it will be possible to account for changes in macroporosity.

Bibliography

[1] Adhikari B.R. (1987)
An Assesment of Requirement in the Flooded Rice Cultivation in the River Terraces of Nepal and its Implications on Water Management.
A Master of Science Thesis, Faculty of Graduate School, of Cornell University, N.Y, U.S.A.

[2] Ahuja L.R and Ross J.D (1983)
A new Green-Ampt Model for Infiltration through a Surface Seal"
Proceedings; National Conference on Advances in Infiltration. ASAE publication (11-83):132-146

[3] Amerman C.R. (1983) *Infiltration Measurement*
Proceedings; National Conference on Advances in Infiltration. ASAE publication (11-83):201-214

[4] Barraclough D., Hyden M.J. and Davies G.P (1983)
Fate of Fertilizer Nitrogen Applied to Grasslands, (I): Field Leaching Results
J. Soil Sci. 34:483-497

[5] Bauer S.W. (1974)
A Modified Horton Equation for Infiltration During Intermittent

Rainfall
J. Hydrological Sciences Bulletin XIX(26): 219-225

[6] Beven K. and Germann P. (1982)
Macropores and Water Flow in Soil
J. Water Resources Res. 18:1331-1325

[7] Bouma J. (1981)
Soil Morphology and Preferential Flow along Macropores
J. Agricultural Water Management 3:235-250

[8] Bouma J., Belmaus C. Dekker L.W and Jeurissen W.J.M (1983)
Assessing the Suitability of Soils with Macropores for Surface Liquid Disposal
J. Environ. Qual. 12:305-310

[9] Bower H. (1978)
Groundwater Hydrology
McGraw Hill, Inc.

[10] Cedergren H.R (1977)
Seepage, Drainage and Flow nets
John Wiley and Sons

[11] Chong S.K. and Green R.C (1983)
Sorptivity and its Applications
Proceedings; National Conference on Advances in Infiltration. ASAE publication (11-83):82-91

[12] Chow V.T, Maidment D.R. and Mays L.W. (1988)
Applied Hydrology
Mc Graw-Hill inc.

[13] Clemens A.J. (1983)
Infiltration Equations for Border Irrigation Models
Proceedings; National Conference on Advances in Infiltration. ASAE publication (11-83):266-274

[14] Clemens A.J and Dedrick A.R. (1981)
Estimating Distribution Uniformity in Level Basins
TRANS. ASAE 24(5):1177-1180, 1187

[15] Edwards W.M, Van der Ploeg R.R, and Ehler W. (1979)
A Numerical Study of the Effect of Non-capillary Sized Pores Upon Infiltration
J.Soil Sci. Soc. Am. 43: 851-856

[16] Eigel J.D. and More I.D (1983)
Effect of Rainfall Energy on Bare Ground
Proceedings; National Conference on Advances in Infiltration. ASAE publication (11-83):188-200

[17] Freeze R.A. and Cherry J.A. (1979)
Ground Water
Prentice-Hall, inc; Englewood cliffs N.J. 07632

[18] Garrick M., Cunnane C. and Nash J.E. (1978)
A Criterion of Efficiency for Rainfall-Runoff Models
J. Hydrology 36:375-381

[19] Ghosh K. (1980)
Modelling Infiltration
J. Soil Science 130(6):297-302

[20] Haan C.T, Johnson H.P, and Brakensiek D.L (1982)
Hydrologic Modelling of Small Watersheds
An ASAE Monograph Number 5

[21] Hanks R.J and Bowers S.A (1963)
Influence in Variation in the Diffusivity-Water Content Relation on Infiltration
J. Soil Sci. Soc. Am. Proc., 27:263-265

[22] Hansen V.E, Israelsen O.W. and Stringum G.E (1979)
Irrigation Practices and Principles
John Wiley & Sons

[23] Hausenbuiller R.L. (1980)
Soil Science Principles and Practices
Second Edition Wm. C. Brown Company Publisher.

[24] Heermann D.F and Duke H.R. (1983)
Applications in Irrigated and Dryland Agriculture
Proceedings; National Conference on Advances in Infiltration. ASAE publication (11-83):254-265

[25] Horton R.E. (1940)
An Approach Towards Physical Interpretation of Infiltration Capacity
J. Soil Sci. Soc. Am. Proc. 5:399-417

[26] Kaluarachchi J.J. and Panker J.C. (1987)
Effects of Hysteresis With Air Entrapment on Water Flow in the Unsaturated Zone
J. Water resources Res. 23(10): 1967-1976

[27] Kennedy and Neville (1986)
Basic Statistical Methods for Engineers and Scientists
Harper and Row, Publishers, Inc.

[28] Kissel D.E., Ritchie J.T. and Burnett E. (1973)
Chloride Movement in Undisturbed Swelling Clay Soil
J. Soil Sci. Soc. Am. Proc. 37:21-24

[29] Kneal W.R. and White R.E. (1884)
The Movement of Water through Cores of Dry (Cracked) Soil
J. Hydrology 67:361-365

[30] Knight J.H. (1983)
Infiltration Functions from Exact and Approximate Solutions of Richard's Equations
Proceedings; National Conference on Advances in Infiltration.
ASAE publication (11-83):24-33

[31] Miller C.J and Mishra M. (1989)
Modelling of Leakage Through Cracked Clay Liners-I: State of the Art
J. Water Resources Bulletin, 25(3):551-555

[32] Miller C.J and Mishra M. (1989)
Modelling of Leakage Through Cracked Clay Liners-II: A New Perspective
J. Water Resources Bulletin, 25(3):556-563

[33] Morel-Seytoux (1983)
Infiltration affected by Air seal, Crust, ice and various sources of Heterogeneity (Special problems)
Proceedings; National Conference on Advances in Infiltration. ASAE publication (11-83):132-146

[34] Morel-Seytoux H.J and Kanji J. (1974)
Derivation of an Equation of Infiltration
J. Water Res. Research, 10:795-800

[35] Morin J. and Benyamini Y.(1977)
Rainfall Infiltration Into Bare Soils
J. Water Resources Research, 13(5):813-817

[36] Mossbarger W.A. Jr., and Yost R.W. (1989)
Effect of Irrigated Agriculture on water Quality in Corn Belt and Lake States
J. Irrigation and Drainage Engineering, ASCE 115(5):773-790

[37] Nash J.E. and Sutcliffe J,V (1970)
River Flow Forecasting Through Conceptual Models Part1: A discussion of Principles
J. Hydrology 10:282-290

[38] Nelson P.A and Gregory J.D (1988)
Saturated Soil Hydraulic Conductivity J. Water Resources Bulletin, 24(4):743-748

[39] Paine J.D. and Watt W.E (1988)
Impact of Tile Drainage
Hydrologic Modelling Group. Queens University Kingston, Ont., Canada

[40] Philip J.R. (1957)
Theory of Infiltration
J. Soil Science 84:257-264

[41] Philip J.R. and Farrell D.A (1964)
General Solution of the Infiltration-Advance Problem in Irrigation Hydraulics
J. Geophys. Res., 69:621-631

[42] Rawls W.J, Onstad C.A and Richardson H.H. (1980)
Residual and Tillage Effects on SCS Runoff Curve Numbers.
Trans. of the ASAE 23(2):357-361

[43] Scotter D.R. (1978)
Preferential Solute Movement through Large Soil Voids Some Computation using Simple Theory

J. Australian Journal of Soil Research 16:257-267

[44] Shirmohammadi A., Gish T.J., Magette W.L. and Lehman D.A. (1989)
"Theoretical Characterization of Preferential flow" ASAE paper No. 89-2576, ASAE, St. Joseph, MI 49085-9659

[45] Shirmohammadi A. and Skaggs R.W. (1985)
"Predicting Infiltration for Shallow Water Table Soils with Different Surface Covers." Transactions of ASAE, 28(6):1829-1837

[46] Singh V.P and Buapeng S. (1977)
Effect of Rainfall-Excess Determination on Runoff Computation
J. Water Resources Res. 13(3):499-513

[47] 31. Skaggs R.W (1982)
Infiltration
Hydrologic Modeling of Small Watersheds An ASAE Monograph number 5 121-166
Edited by Haan C.T, Johnson H.P, and Brakensiek D.L

[48] Skaggs R.W. and Miller D.E (1983)
Soil Water
Design and Operation of Farm Irrigation System, An ASAE Monograph Number 3.

[49] Smith M.S., Thomas G.W., White R.E. and Ritonga D. (1985)
Transport of Escherichia Coli through Intact and Disturbed column of Soil
J. Environmental Quality 14:87-91

[50] Springer E.P. and Cundy T.W. (1987)
Field Scale Evaluation of Infiltration Parameters From Soil Texture for Hydrologic Analysis
J. Water Resources Research 23(2):325-334

[51] Talsma T. (1969)
In-situ Measurement of Sorptivity
Australian J. Soil Res.
7:269-276

[52] Thomas D.B, Edwards K.A, Barber R.G and Hogg I.G.G (1981)
Runoff, Erosion and Conservation in a Representative Catchment in Machakos District, Kenya
J. Tropical Agricultural Hydrology 395-417

[53] Thomas G.W. and Philip R.E. (1979)
Consequences of Water Movement in Macropores
J. Environ. Qual. 8:149-152

[54] Thorntwaite G.W and Holzman B. (1942)
Measurement of Evaporation From Land and Water Sources
USDA Technical Bulletin No. 817

[55] Turbak A.S and Morel-Seytoux H.J (1988)
Analytical Solutions For Surface Irrigation
J. Irrigation and Drainage Engineering, ASCE, 114(1):48-59

[56] UNESCO (1987)
Manual on Drainage in Urbanized Areas
Edited by Geiger W.F. Marsalek J, Rawls W.J and Zuidema F.C

[57] Walker W.R. and Willardson L.S (1983)
Infiltration Measurement for Simulating Furrow Irrigation

Proceedings; National Conference on Advances in Infiltration. ASAE publication (11-83):241-240

[58] White R.E (1985)
The Influence of Macropores on the Transport of Dissolved and Suspended Matter Through Soil
J. Advances in Soil Science,
Springer-Verlag, New York Inc., 95-120

[59] White R.E, Wellings S.R, Bell J.P (1983)
Seasonal Variation in Nitrate Leaching in Structured Clay Soils Under Mixed Land Use.
J. Agricultural Water Management, 7:391-410

[60] Yamada T and Kobayashi M. (1988)
Kinematic Wave Characteristics and New Equations of Unsaturated Infiltration
J. Hydrology 102:257-266

[61] Yoder R.D (1986)
The Performance of Farmer-Managed Irrigation Systems in the Hills of Nepal
A Doctor of Philosophy Thesis, Faculty of Graduate School, of Cornell University , N.Y., U.S.A

[62] Zegelin S.J. and White I. (1982)
Design for a Field Sprinkler Infiltrometer
J. Soil Science Society of America, 46:1129-1133

Appendix A

OBSERVED RUNOFF, AND INFILTRATION RATES

Table A.1: Observed data, Runoff and Infiltration Rates

Zero Macropores			*2 Macropores*			*8 Macropores*		
Time (hr)	Runoff (mm/hr)	Infil. (mm/hr)	Time (hr)	Runoff (mm/hr)	Infil. (mm/hr)	Time (hr)	Runoff (mm/hr)	Infil. (mm/hr)
.13	4.4	55.6	.15	4.5	55.5	.17	4.5	55.5
.15	9.2	50.8	.17	11.1	48.9	.18	11.1	48.9
.17	14.1	45.9	.18	15.3	44.7	.20	15.6	44.4
.18	18.0	42.0	.20	19.5	40.5	.22	18.9	41.1
.22	27.6	32.4	.22	25.5	34.5	.23	22.5	37.5
.23	30.0	30.0	.23	29.1	20.9	.25	25.8	24.2
.25	36.0	24.0	.25	33.0	27.0	.27	28.8	21.2
.27	39.0	21.0	.27	36.0	24.0	.28	31.5	28.5
.28	42.0	18.0	.28	39.0	21.0	.30	36.0	24.0
.50	45.0	15.0	.30	42.0	18.0	.35	39.0	21.0
1.00	48.0	12.0	.42	45.0	15.0	.42	42.0	18.0
1.12	30.0		1.00	45.0	15.0	1.00	42.0	18.0
1.42	6.0		1.12	16.2		1.08	21.0	
1.67	0.3		1.25	2.4		1.33	0.6	

Table A.2: Observed data, Runoff and Infiltration Rates

12 Macropores			*14 Macropores*			*16 Macropores*		
Time (hr)	Runoff (mm/hr)	Infil. (mm/hr)	Time (hr)	Runoff (mm/hr)	Infil. (mm/hr)	Time (hr)	Runoff (mm/hr)	Infil. (mm/hr)
.20	15.0	45	.18	0.0	60.0	.20	16.5	43.5
.22	19.2	40.8	.20	13.5	46.5	.22	20.1	39.9
.23	23.7	36.3	.22	18.0	42.0	.23	22.5	37.5
.25	25.2	34.8	.23	20.7	39.3	.25	24.9	35.1
.27	29.1	30.9	.25	23.4	36.6	.27	26.7	33.3
.28	30.0	30.0	.27	25.5	34.5	.28	28.5	31.5
.30	31.5	28.5	.28	27.3	32.7	.30	29.7	30.3
.32	33.0	27.0	.30	29.4	30.6	.32	30.0	30.0
.33	34.0	25.5	.32	30.0	30.0	.42	34.2	25.8
.35	36.0	24.00	.45	33.0	27.00	.50	36.6	23.4
.42	37.5	22.5	.58	33.0	27.0	.60	36.6	23.4
.50	39.0	21.0	.75	34.8	25.2	.75	36.6	23.4
.83	39.0	21.0	1.00	36.0	24.0	.83	36.6	23.4
1.00	39.0	21.0	1.08	18.3		.92	36.6	23.4
1.08	18.6		1.25	1.5		1.00	36.6	
1.20	3.0		1.37	.3		1.07	16.8	
1.33	0.9					1.17	2.4	

Table A.3: Observed data, Runoff and Infiltration Rates

			20 Macropores		
Time (hr)	Runoff (mm/hr)	Infil. (mm/hr)	Time (hr)	Runoff (mm/hr)	Infil. (mm/hr)
.17	3.6	56.4	.17	4.8	55.2
.20	11.4	48.6	.20	15.3	44.7
.23	20.7	39.3	.25	21.6	38.4
.25	24.3	35.7	.28	27.0	33.0
.28	27.9	32.1	.33	31.8	28.2
.38	33.0	27.0	.50	36.3	23.7
.50	33.9	26.1	.70	36.3	23.7
.58	34.8	25.2	.83	36.3	23.7
.67	35.4	24.6	1.00	36.9	23.1
.80	36.0	24.0	1.17	2.4	
.87	36.3	23.7	1.50	0.0	
.93	36.6	23.4			
1.00	36.6	23.4			
1.12	9.3				
1.25	0.9				
1.35	0.4				

Table A.4: Observed data, Runoff and Infiltration Rates

22 Macropores			*24 Macropores*		
Time (hr)	Runoff (mm/hr)	Infil. (mm/hr)	Time (hr)	Runoff (mm/hr)	Infil. (mm/hr)
.17	3.3	56.7	.18	9.0	51.0
.22	16.8	43.2	.22	16.8	43.0
.25	21.6	38.4	.25	22.2	37.8
.30	26.7	33.3	.30	26.7	33.3
.33	28.5	31.5	.33	29.7	30.3
.42	30.0	30.0	.42	31.2	28.8
.50	31.2	28.8	.50	31.8	28.2
.58	31.8	28.2	.58	32.4	27.6
.67	32.4	27.6	.67	32.7	27.3
.75	32.4	27.6	.75	32.7	27.3
.83	32.7	27.3	.85	33.3	26.7
.92	33.0	27.0	.93	34.2	25.8
1.00	33.3	26.7	1.00	34.2	25.8
1.18	1.2		1.08	13.5	
			1.17	1.2	
			1.42	0.3	

Appendix B

OBSERVED TILE FLOW

Table B.1: Observed Tile Flow (mm/hr)

Time (hr)	*Number of Macropores*				
	0	2	8	12	14
.50	0.0				
.55	0.0				0
.60	4.5			0	7.2
.65	6.0		0	6.9	14.0
0.7	7.0		7.5	10.0	15.0
.75	7.8	0	9.0	12.0	16.8
0.8	8.0	6.0	10.0	14.0	18.0
0.9	9.0	9.0	12.5	15.0	18.6
1.0	9.0	10.0	13.5	15.3	19.2
1.1	8.4	9.3	13.6	15.0	18.3
1.2	7.2	7.5	10.8	12.0	14.4
1.3	5.7	7.0	7.5	8.0	10.0
1.4	4.5	5.4	6.0	7.5	7.2
1.5	3.6	4.0	5.5	6.0	6.0
1.60	3.5	4.0	4.8	5.8	5.5
1.70	3.1	3.9	4.5	5.1	4.8
1.80	3.0	3.0	4.2	4.5	4.2
2.00	2.7	2.7	3.6	3.9	3.9

Table B.2: Observed data, Tile Flow (mm/hr)

Time (hr)	Number of Macropores				
	16	18	20	22	24
.50	0.0			0	0
.55	4.5			7.5	7.2
.60	10.5	0	0	11.7	13.8
.65	13.0	9.9	6.0	16.5	17.4
0.7	14.4	12.0	12.0	18.0	19.0
.75	15.9	14.5	15.0	19.0	20.0
0.8	16.8	15.0	17.0	19.5	21.0
0.9	17.4	15.9	18.6	20.1	21.3
1.0	18.0	16.5	19.2	21.0	21.6
1.1	16.5	15.9	16.0	17.0	21.6
1.2	12.6	12.0	13.8	14.7	16.8
1.3	8.7	9.0	9.0	10.5	12.0
1.4	7.5	8.0	8.0	8.5	8.7
1.5	6.9	7.2	7.2	7.8	7.8
1.60	6.5	6.5	6.5	6.5	7.5
1.70	6.0	6.0	6.0	5.7	6.9
1.80	5.1	5.7	5.1	5.7	6.0
2.00	4.8	5.4	5.1	5.7	5.7